Supplementary Information

Peptoid-based Reprogrammable Template for Cell-Permeable Inhibitors of Protein–Protein Interactions

Yasuhiro Fukuda,[a] Marin Yokomine,[a] Daisuke Kuroda,[ab] Kouhei Tsumoto,[abc] Jumpei Morimoto,*[a] and Shinsuke Sando*[ab]

a. *Department of Chemistry and Biotechnology, Graduate School of Engineering, The University of Tokyo, 7-3-1 Hongo, Bunkyo-ku, Tokyo, 113-8656, Japan.*

b. Department of Bioengineering, Graduate School of Engineering, The University of Tokyo, 7-3-1 Hongo, Bunkyo-ku, Tokyo, 113-8656, Japan

c. *Institute of Medical Science, The University of Tokyo, 4-6-1, Shirokanedai, Minato-ku, Tokyo, 108-8639, Japan*

Email: jmorimoto@chembio.t.u-tokyo.ac.jp, ssando@chembio.t.u-tokyo.ac.jp

Table of Contents

Materials and Methods

Abbreviations for chemical compounds.

TEAA, Triethylammonium acetate; DMSO, Dimethylsulfoxide; DMF, *N*,*N*-Dimethylformamide; Fmoc, 9-Fluorenylmethyloxycarbonyl; COMU, (1-Cyano-2-ethoxy-2-oxoethylideneaminooxy)dimethylamino-morpholino-carbenium hexafluorophosphate; EEDQ, 2-Ethoxy-1-ethoxycarbonyl-1,2-dihydroquinoline; TFA, Trifluoroactic acid; DCM, Dichloromethane; DIPEA, *N*,*N*-Diisopropylethylamine; NMP, *N*-Methylpyrrolidone; TMOF, Trimethyl orthoformate; Ns, *o*-Nitrobenzenesulfonyl; DIAD, Diisopropyl azodicarboxylate; TMP, 2,4,6-Trimethylpyridine; DBU, 1,8-Diazabicyclo[5.4.0]undec-7-ene; DIC, *N*,*N'*-Diisopropylcarbodiimide ; HOBt, 1-Hydroxybenzotriazole

General remarks for synthesis.

Chemicals and solvents used in this study were purchased from commercial suppliers and used without further purification. Preparative high performance liquid chromatography (HPLC) was performed on a Prominence HPLC system (Shimadzu) with a 5C_{18}-MS-II column (Nacalai tesque, 10 mm I.D.×150 mm, 34355-91). Analytical HPLC was performed on a Prominence HPLC system with a 5C_{18}-AR-II column (Nacalai tesque, 4.6 mm I.D.×150 mm, 38144-31). HRMS data was obtained using micrOTOF II (Bruker Daltonics). Analytical ultra high performance liquid chromatography (UHPLC) was performed on a Nexera-i (Shimadzu) with a Shim-pack Velox C18 column (Shimadzu, 1.8 μM, 2.1 mm×50 mm, 227-32007-02).

General procedures for synthesis of oligo-NSAs with piperazinyl C-termini.

Trityl chloride resin (#A00220, Watanabe Chemical Industries) was used for synthesis. Objective oligomers were synthesized on resin and cleaved as previously reported.[1] Before cleaving the oligomers from resin, acetyl groups adducted to indole were removed by reduction using $NaBH_4$. Detailed procedures about each reaction step are described below. The crude product was dissolved in acetonitrile and water, and purified by a reversed phase column on HPLC using acetonitrile and 100 mM TEAA (pH 7.0) as solvents. After lyophilization, obtained compounds were dissolved in DMSO and quantified from UV absorbance derived from indole (ε = 5360 $cm^{-1}\cdot M^{-1}$ at 280 nm determined from 3-hydroxymethyindole) or 6-choloroindole (ε = 4230 $cm^{-1}\cdot M^{-1}$ at 286 nm determined from 6-chloro-3-hydroxymethyindole). Yields were determined by comparing with the amount of the first Fmoc-Ala-OH loaded on resin quantified as previously reported.[1] The purified products were analyzed on a reversed phase column by HPLC and

ESI-TOF MS.

General procedures for synthesis of oligo-NSAs with amide C-termini.

Fmoc-protected Sieber amide resin (#A00258, Watanabe Chemical Industries) was used for synthesis. The resin was swelled with DMF for 30 min and then Fmoc protecting group was removed by treatment with 20% piperidine/DMF (3 min and 12 min). Coupling reaction of the first Fmoc-Ala-OH was conducted using COMU as a coupling reagent. After deprotection of Fmoc group, an N-substituent was introduced by reductive amination. Objective oligomers were synthesized on resin as previously reported[1] by repeating the cycle of coupling of Fmoc-Ala-OH using EEDQ as a coupling reagent, deprotection of Fmoc, and introduction of an N-substituent by reductive amination. For 2-methoxyethyl group, 2-hydroxyethyl group, and 4-chlorophenylethyl group, substituents were introduced on resin using alcohols by Fukuyama-Mitsunobu reaction.[2] For residues with N-methyl substituents, coupling reaction of Fmoc-*N*-Me-Ala-OH was conducted instead of introducing an N-substituent by reductive alkylation or Fukuyama-Mitsunobu reaction. Before cleaving oligomers from resin, acetyl groups adducted to indole were removed by reduction using $NaBH_4$. Detailed procedures about each reaction step are described below. The oligomers were cleaved by treatment of the resin with 1% TFA/DCM for 10 s. The solution was transferred to a glass vial containing pyridine/methanol to quench TFA. This cleavage process was repeated five times. The resin was washed with methanol three times and the methanol solutions were collected in the glass vial. The solvents were removed under reduced pressure. The crude product was dissolved in acetonitrile and water, and purified by a reversed phase column on HPLC using acetonitrile and 100 mM TEAA (pH 7.0) as solvents. After lyophilization, obtained compounds were dissolved in DMSO and quantified from UV absorbance derived from indole (ε = 5360 $cm^{-1}\cdot M^{-1}$ at 280 nm determined from 3-hydroxymethyindole), 6-choloroindole (ε = 4230 $cm^{-1}\cdot M^{-1}$ at 286 nm determined from 6-chloro-3-hydroxymethyindole), or 5-choloroindole (ε = 4300 $cm^{-1}\cdot M^{-1}$ at 288 nm determined from 5-chloro-3-hydroxymethyindole). Yields were determined by comparing with the loading amount of the resin. The purified products were analyzed on a reversed phase column by HPLC and ESI-TOF MS.

Coupling reaction using COMU.

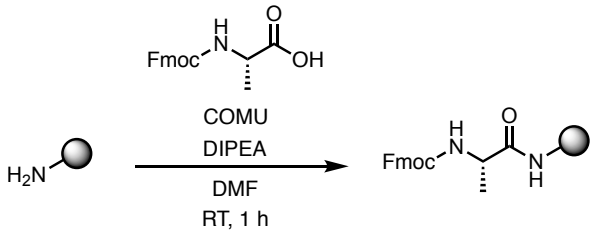

Resin-bound primary amine was coupled with Fmoc-Ala-OH as follows. First, resin was washed with DMF three times. Then, a DMF solution of Fmoc-Ala-OH (4 equiv., 0.2 M), COMU (4 equiv., 0.2 M) and DIPEA (8 equiv., 0.4 M) was added to the resin and the reaction vessel was shaken for 1 h. After the solution was removed, the resin was washed with DMF three times.

Coupling reaction using EEDQ.

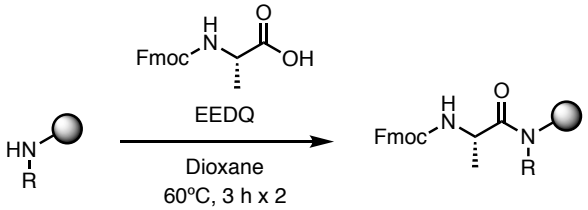

Resin-bound secondary amine was coupled with Fmoc-Ala-OH as follows. First, resin was washed with dioxane three times. Fmoc-Ala-OH (4 equiv.) and EEDQ (4 equiv.) were dissolved in dioxane to prepare 0.2 M solution and the mixture was shaken. After 30 min, the solution was added to the resin and the reaction vessel was shaken for 3 h at 60ºC. This coupling reaction was repeated once more when the *N*-terminal substituent on the resin is larger than methyl. After the reaction, the resin was washed with dioxane and DMF three times each.

Introduction of a substituent on resin-bound primary amine by reductive amination.

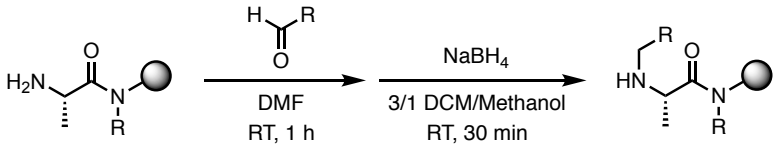

Resin was washed with DMF three times, then incubated with 1 M (20 equiv.) of an aldehyde solution in DMF for 1 h. The solution was filtered off and the resin was quickly washed with DMF and DCM twice each. A 3/1 DCM/methanol solution (20 μL/μmol of loading amount of resin) and 10 equiv. of $NaBH_4$ were added to the resin and shaken for 30 min with the reaction vessel standing and open to the atmosphere. The resin was washed with methanol five times then with DCM and DMF three times each.

Introduction of an indolylmethyl group derivative on resin-bound primary amine by reductive amination.

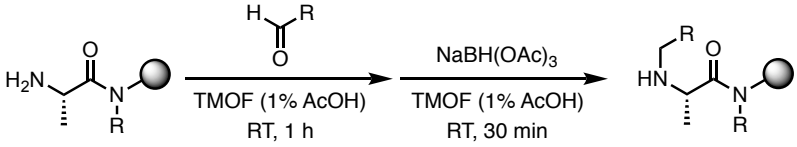

Resin was washed with TMOF three times, then incubated with a suspension of aldehyde (10 equiv.) in

TMOF (20 μL/μmol of loading amount of resin) with 1% acetic acid as an additive for 1 h. 10 equiv. of $NaBH(OAc)_3$ was added to the reaction mixture and shaken for additional 30 min. The resin was washed with methanol five times then with DMF three times.

Introduction of an N-substituent on resin-bound primary amine by Fukuyama- Mitsunobu reaction.

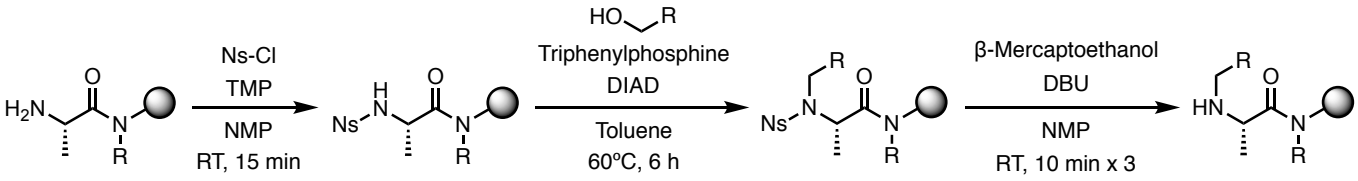

Resin was washed with NMP three times and then incubated with a solution of Ns-Cl (4 equiv., 0.1 M) and TMP (10 equiv., 0.25 M) in NMP for 15 min. The solution was filtered off and the resin was washed with NMP and toluene three times each. A solution of alcohol (8 equiv., 0.8 M) and triphenylphosphine (4 equiv., 0.4 M) in toluene was added to the resin, and a solution of DIAD (4 equiv., 0.4 M) in toluene was added dropwise to give a final concentration of 0.4 M of alcohol, 0.2 M of triphenylphosphine and 0.2 M of DIAD. The reaction vessel was capped and allowed to shake for 6 h at 60ºC. After the resin was washed with toluene and DMF three times each, *o*-NBS groups were removed by the treatment with a solution of β-mercaptoethanol (8 equiv., 0.4 M) and DBU (4 equiv., 0.2 M) in NMP for 10 min. This deprotection process was repeated twice more and the resin was washed with DMF three times.

Acetylation of N-terminal amine.

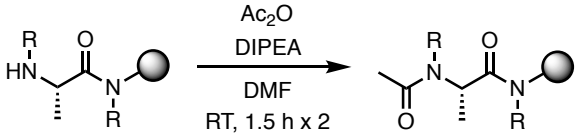

Resin was washed with DMF three times. A DMF solution of acetic anhydride (10 equiv., 0.5 M) and DIPEA (20 equiv., 1 M) was added to the resin and the reaction vessel was shaken for 1.5 h. This procedure was repeated once more, and the resin was washed with DMF three times.

Removal of adducted acetyl group on indole.

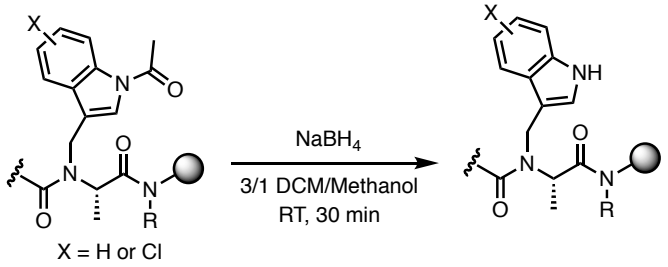

Resin was washed with DCM three times. A solution of 3/1 DCM/methanol (20 μL/μmol of loading amount of resin) and 10 equiv. of $NaBH_4$ was added to the resin and shaken for 30 min with the reaction vessel standing and open to the atmosphere. The resin was washed with methanol five times then with DCM three times.

Synthesis of oligo-NSA 1–9.

Synthesis of oligo-NSA 1.

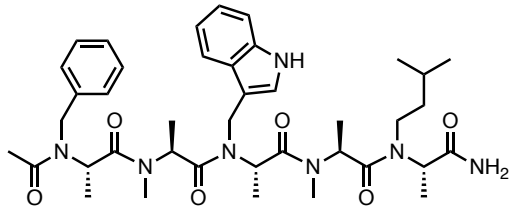

41 mg of Sieber amide resin (0.48 mmol/g, 20 μmol) was used for synthesis. Fmoc-Ala-OH, Fmoc-*N*-Me-Ala-OH, isovaleraldehyde, indole-3-carboxaldehyde and benzaldehyde were used as submonomers. Yield: 6%. HRMS (ESI-TOF MS) m/z: $[M + Na]^+$ Calcd for $C_{40}H_{57}N_7NaO_6^+$ 754.4263; Found 754.4254.

Synthesis of oligo-NSA 1-Pip.

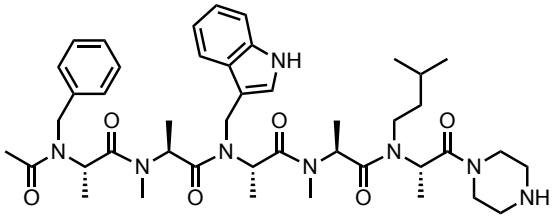

40 mg of trityl chloride resin (1.96 mmol/g, 78 μmol) was used for synthesis. Fmoc-Ala-OH, Fmoc-*N*-Me-Ala-OH, isovaleraldehyde, indole-3-carboxaldehyde and benzaldehyde were used as submonomers. After loading first Fmoc-alanine, the loading amount was determined as 1.2 mmol/g. Yield:

56%. HRMS (ESI-TOF MS) m/z: $[M + H]^+$ Calcd for $C_{44}H_{65}N_8O_6^+$ 801.5022; Found 801.5029.

Synthesis of oligo-NSA 2.

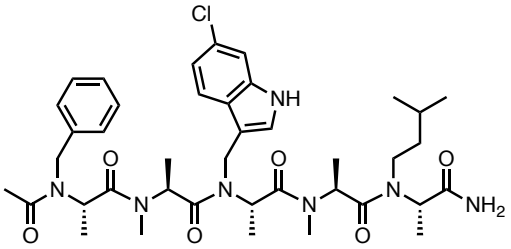

40 mg of Sieber amide resin (0.48 mmol/g, 19 μmol) was used for synthesis. Fmoc-Ala-OH, Fmoc-*N*-Me-Ala-OH, isovaleraldehyde, 6-chloroindole-3-carboxaldehyde and benzaldehyde were used as submonomers. Yield: 7%. HRMS (ESI-TOF MS) m/z: $[M + Na]^+$ Calcd for $C_{40}H_{56}ClN_7NaO_6^+$ 788.3873; Found 788.3893.

Synthesis of oligo-NSA 3.

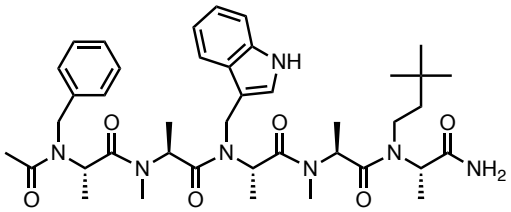

41 mg of Sieber amide resin (0.48 mmol/g, 20 μmol) was used for synthesis. Fmoc-Ala-OH, Fmoc-*N*-Me-Ala-OH, 3,3-dimethylbutyraldehyde, indole-3-carboxaldehyde and benzaldehyde were used as submonomers. Yield: 6%. HRMS (ESI-TOF MS) m/z: $[M + Na]^+$ Calcd for $C_{41}H_{59}N_7NaO_6^+$ 768.4419; Found 768.4436.

Synthesis of oligo-NSA 4.

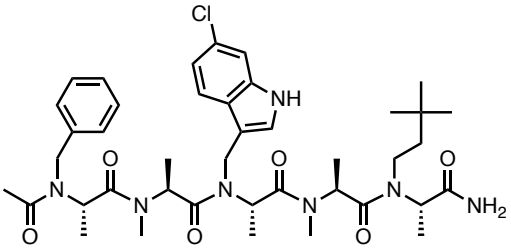

83 mg of Sieber amide resin (0.48 mmol/g, 40 μmol) was used for synthesis. Fmoc-Ala-OH, Fmoc-*N*-Me-Ala-OH, 3,3-dimethylbutyraldehyde, 6-chloroindole-3-carboxaldehyde and benzaldehyde were used as submonomers. Yield: 8%. HRMS (ESI-TOF MS) m/z: $[M + Na]^+$ Calcd for $C_{41}H_{58}ClN_7NaO_6^+$ 802.4029; Found 802.4027.

Synthesis of oligo-NSA 5.

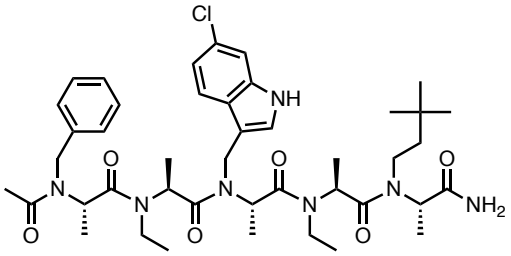

100 mg of Sieber amide resin (0.48 mmol/g, 48 μmol) was used for synthesis. Fmoc-Ala-OH, acetaldehyde, 3,3-dimethylbutyraldehyde, 6-chloroindole-3-carboxaldehyde and benzaldehyde were used as submonomers. Yield: 2%. HRMS (ESI-TOF MS) m/z: $[M + Na]^+$ Calcd for $C_{43}H_{62}ClN_7NaO_6^+$ 830.4342; Found 830.4331.

Synthesis of oligo-NSA 5-Pip.

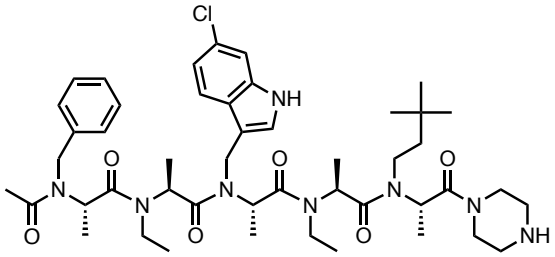

80 mg of trityl chloride resin (1.96 mmol/g, 156 μmol) was used for synthesis. Fmoc-Ala-OH, acetaldehyde, 3,3-dimethylbutyraldehyde, 6-chloroindole-3-carboxaldehyde and benzaldehyde were used as submonomers. After loading first Fmoc-alanine, the loading amount was determined as 1.2 mmol/g. Yield: 41%. HRMS (ESI-TOF MS) m/z: $[M + H]^+$ Calcd for $C_{47}H_{70}ClN_8O_6^+$ 877.5101; Found 877.5094.

Synthesis of oligo-NSA 5-Rv.

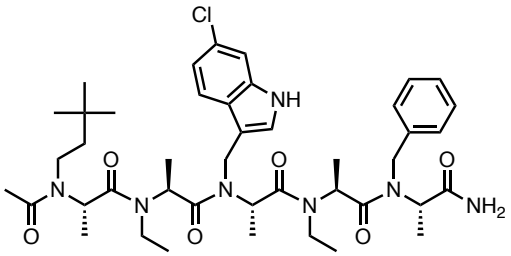

99 mg of Sieber amide resin (0.48 mmol/g, 48 μmol) was used for synthesis. Fmoc-Ala-OH, acetaldehyde, benzaldehyde, 6-chloroindole-3-carboxaldehyde and 3,3-dimethylbutyraldehyde were used as submonomers. Yield: 2%. HRMS (ESI-TOF MS) m/z: $[M + Na]^+$ Calcd for $C_{43}H_{62}ClN_7NaO_6^+$ 830.4342; Found 830.4304.

Synthesis of oligo-NSA 6.

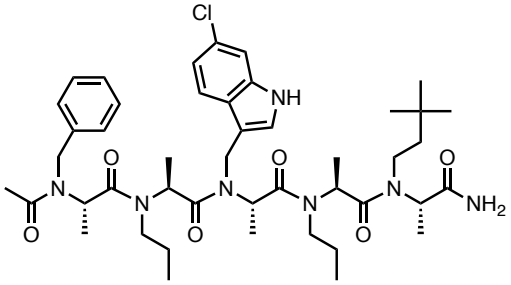

34 mg of Sieber amide resin (0.48 mmol/g, 16 μmol) was used for synthesis. Fmoc-Ala-OH, Propionaldehyde, 3,3-dimethylbutyraldehyde, 6-chloroindole-3-carboxaldehyde and benzaldehyde were used as submonomers. Yield: 3%. HRMS (ESI-TOF MS) m/z: $[M + Na]^+$ Calcd for $C_{45}H_{66}ClN_7NaO_6^+$ 858.4655; Found 858.4633.

Synthesis of oligo-NSA 7.

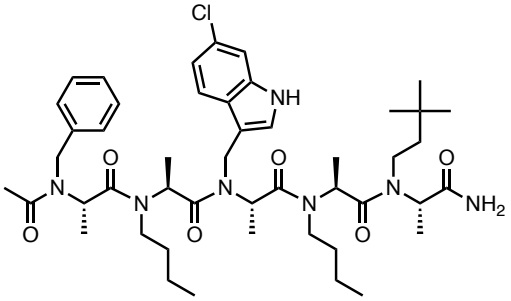

34 mg of Sieber amide resin (0.48 mmol/g, 16 μmol) was used for synthesis. Fmoc-Ala-OH, n-butylaldehyde, 3,3-dimethylbutyraldehyde, 6-chloroindole-3-carboxaldehyde and benzaldehyde were used as submonomers. Yield: 2%. HRMS (ESI-TOF MS) m/z: $[M + Na]^+$ Calcd for $C_{47}H_{70}ClN_7NaO_6^+$ 886.4968; Found 886.4938.

Synthesis of oligo-NSA 8.

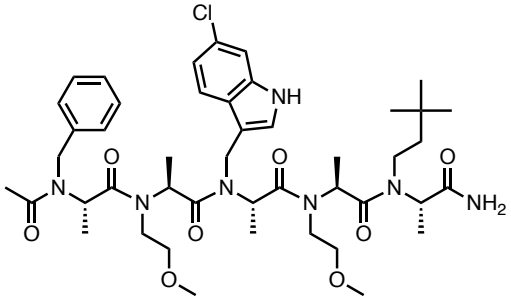

100 mg of Sieber amide resin (0.48 mmol/g, 48 μmol) was used for synthesis. Fmoc-Ala-OH, 2-methoxyethanol, 3,3-dimethylbutyraldehyde, 6-chloroindole-3-carboxaldehyde and benzaldehyde were

used as submonomers. Yield: 5%. HRMS (ESI-TOF MS) m/z: $[M + Na]^+$ Calcd for $C_{45}H_{66}ClN_7NaO_8^+$ 890.4554; Found 890.4511.

Synthesis of oligo-NSA 9.

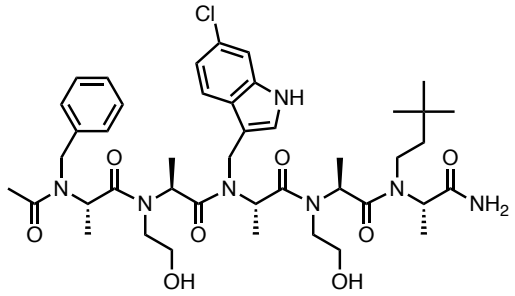

100 mg of Sieber amide resin (0.48 mmol/g, 48 μmol) was used for synthesis. Fmoc-Ala-OH, 2-[[*tert*-butyl(dimethyl)silyl]oxy]ethanol, 3,3-dimethylbutyraldehyde, 6-chloroindole-3-carboxaldehyde and benzaldehyde were used as submonomers. Before removal of acetyl group and cleavage from resin, *tert*-butyldimethylsilyl protecting groups were removed by treatment of the resin with 0.1 M tetrabutylammonium fluoride in 9/1 DMF/THF for 2 h. Yield: 1%. HRMS (ESI-TOF MS) m/z: $[M + Na]^+$ Calcd for $C_{43}H_{62}ClN_7NaO_8^+$ 862.4241; Found 862.4199.

Synthesis of oligo-NSA S1–S7.

Synthesis of oligo-NSA S1.

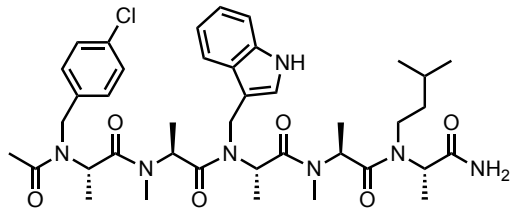

40 mg of Sieber amide resin (0.48 mmol/g, 19 μmol) was used for synthesis. Fmoc-Ala-OH, Fmoc-*N*-Me-Ala-OH, isovaleraldehyde, indole-3-carboxaldehyde and 4-chlorobenzaldehyde were used as submonomers. Yield: 4%. HRMS (ESI-TOF MS) m/z: $[M + Na]^+$ Calcd for $C_{40}H_{56}ClN_7NaO_6^+$ 788.3873; Found 788.3897.

Synthesis of oligo-NSA S2.

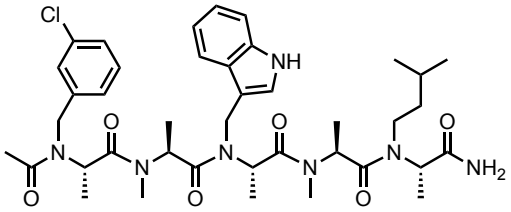

40 mg of Sieber amide resin (0.48 mmol/g, 19 μmol) was used for synthesis. Fmoc-Ala-OH, Fmoc-*N*-Me-Ala-OH, isovaleraldehyde, indole-3-carboxaldehyde and 3-chlorobenzaldehyde were used as submonomers. Yield: 4%. HRMS (ESI-TOF MS) m/z: $[M + Na]^+$ Calcd for $C_{40}H_{56}ClN_7NaO_6^+$ 788.3873; Found 788.3887.

Synthesis of oligo-NSA S3.

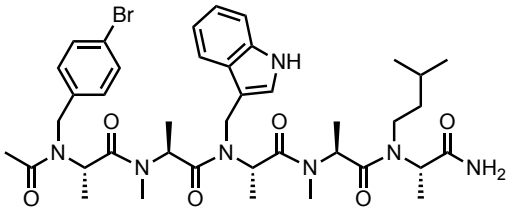

40 mg of Sieber amide resin (0.48 mmol/g, 19 μmol) was used for synthesis. Fmoc-Ala-OH, Fmoc-*N*-Me-Ala-OH, isovaleraldehyde, indole-3-carboxaldehyde and 4-bromombenzaldehyde were used as submonomers. Yield: 2%. HRMS (ESI-TOF MS) m/z: $[M + Na]^+$ Calcd for $C_{40}H_{56}BrN_7NaO_6^+$ 832.3368; Found 832.3376.

Synthesis of oligo-NSA S4.

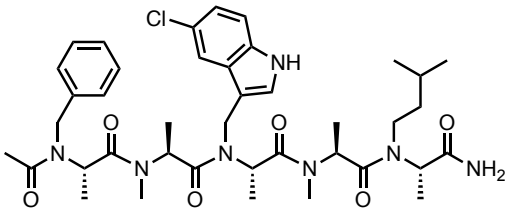

40 mg of Sieber amide resin (0.48 mmol/g, 19 μmol) was used for synthesis. Fmoc-Ala-OH, Fmoc-*N*-Me-Ala-OH, isovaleraldehyde, 5-chloroindole-3-carboxaldehyde and benzaldehyde were used as submonomers. Yield: 16%. HRMS (ESI-TOF MS) m/z: $[M + Na]^+$ Calcd for $C_{40}H_{56}ClN_7NaO_6^+$ 788.3873; Found 788.3895.

Synthesis of oligo-NSA S5.

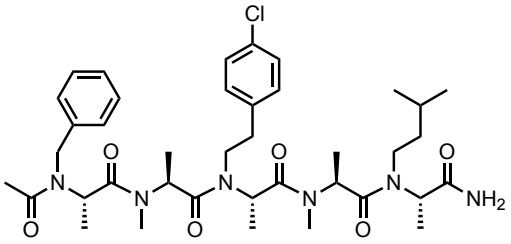

40 mg of Sieber amide resin (0.48 mmol/g, 19 μmol) was used for synthesis. Fmoc-Ala-OH, Fmoc-*N*-Me-Ala-OH, isovaleraldehyde, 2-(4-chlorophenyl)ethanol and benzaldehyde were used as submonomers. Yield: 48%. HRMS (ESI-TOF MS) m/z: $[M + Na]^+$ Calcd for $C_{39}H_{57}ClN_6NaO_6^+$ 763.3920; Found 763.3951.

Synthesis of oligo-NSA S6.

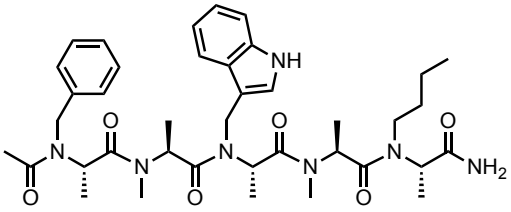

41 mg of Sieber amide resin (0.48 mmol/g, 20 μmol) was used for synthesis. Fmoc-Ala-OH, Fmoc-*N*-Me-Ala-OH, n-butylaldehyde, indole-3-carboxaldehyde and benzaldehyde were used as submonomers. Yield: 6%. HRMS (ESI-TOF MS) m/z: $[M + Na]^+$ Calcd for $C_{39}H_{55}N_7NaO_6^+$ 740.4106; Found 740.4122.

Synthesis of oligo-NSA S7.

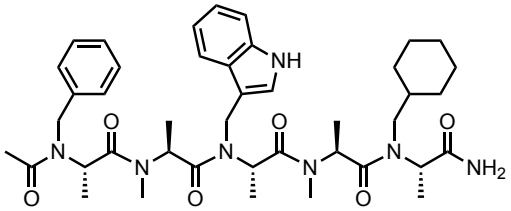

41 mg of Sieber amide resin (0.48 mmol/g, 20 μmol) was used for synthesis. Fmoc-Ala-OH, Fmoc-*N*-Me-Ala-OH, cyclohexanecarboxaldehyde, indole-3-carboxaldehyde and benzaldehyde were used as submonomers. Yield: 7%. HRMS (ESI-TOF MS) m/z: $[M + Na]^+$ Calcd for $C_{42}H_{59}N_7\ NaO_6^+$ 780.4419; Found 780.4431.

Synthesis of fluorescently labeled PMI peptide (Fluorescein-TSFAEYWNLLSP–NH_2, Flu-PMI) for FP assay.

PMI peptide[3] was synthesized by standard Fmoc solid phase peptide synthetic method on a fully automated parallel peptide synthesizer Syro I (Biotage) using Rink Amide-MBHA resin (#A00172, Watanabe Chemical Industries) and Fmoc-amino acids. 50 mg of Rink Amide-MBHA resin (0.48 mol/mg, 24 μmol) was used for synthesis. Coupling reaction was performed with DMF solution of Fmoc-amino acid (4 equiv., 0.2M), COMU (4 equiv., 0.2 M) and DIPEA (8 equiv., 0.4 M). Coupling reaction of 5(6)-carboxyfluorescein was performed manually. DMF solution of 5(6)-carboxyfluorescein (2.5 equiv., 0.1 M), DIC (2.5 equiv., 0.1 M) and HOBt (2.5 equiv., 0.1 M) was added to the resin with continuous shaking overnight. After removing the solution, the resin was washed with DMF three times and incubated with 20% piperidine/DMF for 45 min to remove any side products bearing additional carboxyfluoresceins. After removing the solution, the resin was washed with DMF, methanol and DCM three times each. Peptide was cleaved and deprotected by treating the resin with 95/2.5/2.5 TFA/TIPS/H_2O for 2 h. The solution was transferred to a recovery flask and TFA solution was removed under reduced pressure. Peptide was precipitated by adding diethylether to the flask. The precipitated crude product was dissolved in acetonitrile and water, and purified by a reversed phase column on HPLC using acetonitrile and water containing 0.1% TFA as solvents. The purified product was analyzed on a reversed phase column by HPLC and ESI-TOF MS. HRMS (ESI-TOF MS) m/z: $[M + Na]^+$ Calcd for $C_{89}H_{105}N_{15}NaO_{25}^+$ 1806.7298; Found 1806.7291.

Synthesis of fluorescently labeled MCL-1 BH3 peptide (Fluorescein-KALETLRRVGDGVQRNHE-TAF–NH_2, Flu-MCL-1 BH3) for FP assay.

Flu-MCL-1 BH3 was synthesized using Rink Amide-MBHA resin and purified by almost the same procedures as for Flu-PMI described in the previous section. Until the 11th residue, peptide (DGVQRNHETAF) was synthesized on a fully automated parallel peptide synthesizer Syro I (Biotage) and the subsequent residues were manually synthesized. The purified product was analyzed on a reversed phase column by UHPLC and ESI-TOF MS. HRMS (ESI-TOF MS) m/z: $[M + H]^{2+}$ Calcd for $C_{123}H_{182}N_{36}O_{37}^{2+}$ 1377.6728; Found 1377.6778.

Recombinant expression and purification of MDM2.

Human MDM2, corresponding to residues 17-125, was expressed using pGEX-6P-2 vectors in BL21 (DE3) cells grown in LB medium as previously described.[1] The pGEX-6P-2-MDM2 (17-125) was a gift from Gary Daughdrill (#62063, Addgene plasmid).[4] After the removal of GST tag, the buffer was

exchanged to 50 mM Tris (pH 7.5), 150 mM NaCl, 1 mM EDTA, 5 mM DTT, and MDM2 was purified by size exclusion chromatography. Size exclusion chromatography was performed on an NGC chromatography system (Bio-Rad) with a HiLoad 16/600 Superdex 75 pg column (#28-9893-33, Cytiva). Fractions containing MDM2 were combined and the buffer was exchanged to PBS.

Recombinant expression and purification of MCL-1.

The BAK-binding domain of human MCL-1, corresponding to residues 172-320, was expressed using pGEX-6P-2 vectors in BL21 (DE3) cells grown in LB medium by almost the same procedures as those of MDM-2 expression. The buffer of the purified MCL-1 was exchanged to 25 mM Tris, 150 mM NaCl (pH 7.4 at 25 °C) using a dialysis membrane with 3.5 K molecular weight cut filter.

Fluorescence polarization (FP) binding assay of fluorescently labeled PMI peptide and MCL-1 BH3 peptide.

Serially diluted MDM2 or MCL-1 solutions were mixed with fluorescently labeled PMI peptide (Flu-PMI) (10 nM) or MCL-1 BH3 peptide (Flu-MCL-1 BH3) (20 nM) solutions in 384-well plate to prepare 15 μL of solutions in PBS or TBS (pH 7.4) containing 0.01% Tween 20. As a control, solutions of 10 nM Flu-PMI or 20 nM Flu-MCL-1 BH3 were also prepared. The plate was spun down at 500 × g for 5 min and incubated at room temperature for 1 h. Fluorescence anisotropy (FA) was measured on a plate reader (TECAN, infinite M1000Pro) at 25ºC. Excitation wavelength and emission wavelength were set to 470 nm and 521 nm, respectively. ΔFA values were determined from the average of three measurements of difference between solution with protein and blank (without protein). Dissociation constants (K_D) were calculated using parameters determined by fitting the plot to the Hill equation on ORIGIN (LightStone): $y = y_{min} + (y_{max} - y_{min})/(1 + (K_D/x)^n)$. x, y, and n denote protein concentration, ΔFA, and hill coefficient, respectively.

FP competitive binding assay of oligo-NSA derivatives.

Serially diluted oligo-NSA solutions were mixed with MDM2 (40 nM) and Flu-PMI (10 nM) or MCL-1 (500 nM) and Flu-MCL-1 BH3 (20 nM) solutions in 384-well plate to prepare 15 μL of solutions in PBS or TBS (pH 7.4) containing 0.01% Tween 20. As a control, solutions of 10 nM Flu-PMI without oligo-NSA and MDM2 or 20 nM Flu-MCL-1 BH3 without oligo-NSA and MCL-1 were also prepared. FA was measured following the same procedures in the previous section. ΔFA values were determined from the average of three measurements of difference between solution with protein and oligo-NSAs and blank (without protein and oligo-NSA). IC_{50} values were determined by fitting the plot to the Hill

equation on ORIGIN (LightStone): $y = y_{max} - y_{max}/(1 + (IC_{50}/x)^n)$. x, y, and n denote inhibitor oligomer concentration, ΔFA and hill coefficient, respectively. Inhibition constants (K_i) were calculated using determined K_D of the Flu-PMI and IC_{50} as previously reported.[5]

Cell monolayer permeability assay.

The assay was conducted using Millicell cell culture insert plates (Millipore). The filter area of the plate was 0.7 cm^2. 0.42×10^5 Caco-2 cells (#HTB-37, ATCC) in 400 μL of culture medium (DMEM with high glucose containing 10% Fetal bovine serum (FBS), 1% nonessential amino acids, and 1% penicillin-streptomycin solution) were spread to each insert chamber and 800 μL of the culture medium was added in each well of the receiver plate. The cell culture insert plates were incubated in a 5% CO_2 incubator at 37ºC for 22 days. During the incubation, medium was refreshed twice in a week. After the incubation, the transepithelial electrical resistance in each well was measured to confirm that the value is > 300 W cm^2, which suggest the formation of a cell monolayer. The medium both in apical and basolateral wells was removed using aspirator and an apical chamber and basolateral chamber was washed with 400 μL and 800 μL of transport buffer (HBSS buffer containing 10 mM HEPES (pH 7.4)), respectively. After the wash, an apical chamber and a basolateral chamber was filled with the same buffer solution and the plates were incubated at 37ºC for 30 min. After removing solution in apical and basolateral wells, 420 μL of 10 μM oligo-NSA solution in transport buffer containing 1% DMSO was added to each apical well and 20 μL of the solution was immediately recovered as sample at time zero. 800 μL of transport buffer containing 1% DMSO was added to each basolateral well and the plates were incubated at 37ºC for 3 h. After the incubation, 20 μL and 200 μL of the solution in an apical well and a basolateral well, respectively, were recovered and analyzed by LC-MS/MS. The solution in apical and basolateral wells was removed using aspirator and 400 μL of 300 μM lucifer yellow solution in transport buffer containing 1% DMSO and 800 μL of transport buffer containing 1% DMSO were added to each apical chamber and basolateral chamber, respectively. An apical chamber and basolateral chamber was washed with 400 μL and 800 μL of transport buffer, respectively. After 1 h incubation in 5% CO_2 incubator at 37ºC for 30 min, 200 μL of solution in basolateral chamber was transferred to a 96-well black plate and fluorescence from each well was measured by a plate reader with excitation wavelength of 485 nm and emission wavelength of 538 nm. Wells with 2×10^{-6} cm/sec for lucifer yellow was not recruited. Using the determined concentrations of oligo-NSAs in apical and basolateral wells, the permeability value (P_e) was calculated according to a previous report.[6] Each compound was tested in triplicate or quadruple.

Parallel artificial membrane permeability assay (PAMPA).

The assay was conducted using Gentest Pre-coated PAMPA Plate System (Corning). The filter area of the plate was 0.3 cm^2. 300 μL of 10 μM solution of each oligo-NSA in 5% DMSO/100 mM phosphate buffer (pH 7.4) was added to each donor well in the receiver microplate and 200 μL of 5% DMSO/PBS was added to each of the wells. For oligo-NSA **6** and **7**, 0.1 and 1 μM solution, respectively, were used due to the low aqueous solubility of the compounds. The donor plate was docked on the acceptor well and the plates were incubated on a thermomixer (Eppendorf) for 4 h at 37ºC. After the incubation, oligo-NSAs in acceptor and donor wells were quantitated by LC-MS/MS. Using the determined concentrations of oligo-NSAs in donor and acceptor wells, the permeability value (P_e) was calculated according to a previous report.[6]

Calculation of ALogP values.

ALogP values were calculated using ALogP 2.1 from Virtual Computational Chemistry Lablatory.[7]

Cell culture.

SJSA-1 and SW480 cells were cultured at 37ºC in 5% CO_2 atmosphere in RPMI-1640 supplemented with 10% heat-inactivated FBS and 1% Antibiotic-Antimycotic (#09366-44, Nacalai Tesque).

Evaluation of intracellular levels of p53 and p21 by western blotting.

SJSA-1 or SW480 cells were seeded in 35-mm dishes (3×10^5 cells) and cultured in RPMI-1640 supplemented with 10% FBS and 1% Antibiotic-Antimycotic for 24 h. The medium was replaced, and the cells were treated with oligo-NSA derivatives or Nutlin-3a (#ab144428, Abcam) at an appropriate concentration in RPMI-1640 (10% FBS, 1% Antibiotic-Antimycotic, 0.1% DMSO) for 8 h at 37ºC in 5% CO_2 atmosphere. The cells were washed with PBS twice and lysed with lysis buffer (50 mM Tris-HCl (pH 8.0), 150 mM NaCl, 0.5% sodium deoxycholate, 0.1% sodium dodecyl sulfate, 1% Nonidet P-40, and 1 μg/mL leupeptin) supplemented with 1 mM AEBSF. The cell lysates were passed through 27 gauge needles followed by centrifugation at 12,000 × g for 30 min at 4 ˚C, and then the supernatants were recovered. The total protein concentration of each cell lysate was determined by Bicinchoninic acid (BCA) assay, and then adjusted to the same value. The cell lysates containing 0.6 or 1 μg of total protein were subjected to SDS-PAGE and then transferred to the polyvinylidene difluoride (PVDF) membranes (#IPVH00010, Merck Millipore). The membranes were blocked with Blocking One (#03953-95, Nacalai Tesque) for 1 h. The membranes were incubated with anti-p53 (1:200; #DO-1, Santa Cruz), anti-p21 (1:200; #OP64, Merck), or anti-β-actin (1:3000; #4967, Cell Signaling Technology) antibodies at 4ºC

overnight, followed by horseradish peroxidase conjugated anti-mouse immunoglobulins (1:3000; P0447, Dako) or anti-rabbit immunoglobulins (1:3000; P0488, Dako) secondary antibodies at room temperature for 1 h. The membranes were probed using ImmunoStar LD (#296-69901, Fujifilm Wako Pure Chemical Corporation), and chemiluminescence was detected using Ez-Capture MG AE9300H-CSP (ATTO).

Evaluation of apoptosis-inducing ability by Annexin V assay.

SJSA-1 or SW480 cells were seeded in 12-well tissue culture plates (1×10^5 cells per well), and cultured in RPMI-1640 supplemented with 10% FBS and 1% Antibiotic-Antimycotic for 24 h. The medium was replaced, and the cells were treated with oligo-NSA derivatives or Nutlin-3a at an appropriate concentration in RPMI-1640 (10% FBS, 1% Antibiotic-Antimycotic, 0.1% DMSO) for 48 h at 37ºC in 5% CO_2 atmosphere. Cells were washed with PBS twice. Culture medium and the first wash solution that may contain detached cells were collected. Cells attached to the plate were detached by incubation with TrypLE Express (#12605028, Thermo Fisher) at 37ºC for 5 min, and combined with collected cells in medium and PBS. Cells were collected by centrifugation at 500 × g for 5 min, and then washed with PBS twice. Apoptotic cells were detected by Annexin V-FITC apoptosis detection kit (#15342-54, Nacalai tesque). Cells were suspended in the supplied binding buffer. Annexin V-FITC and propidium iodide (PI) solutions were added to the cell suspensions. The cell suspensions were incubated at room temperature for 15 min in the dark. The suspensions were diluted with the supplied binding buffer and analyzed by flow cytometry (Guava easyCyte, Merck Millipore).

CD studies.

CD spectra of 50 μM oligo-NSAs in 20 mM phosphate buffer (pH 7.4) containing 5% methanol were measured at 25ºC with a CD spectrometer (JASCO, J-1500) using 1 mm path length quartz cell (JASCO, 209J). Data pitch was set to 1 mm. Spectra were averaged from three scans. Spectral baseline was recorded using 20 mM phosphate buffer (pH 7.4) containing 5% methanol. All data points were baseline subtracted, converted to a uniform scale of molar ellipticity per residue and plotted.

NMR spectroscopic studies.

NMR spectra of oligo-NSA **1-Pip** and **5-Pip** were recorded at 15 mM in $CDCl_3$ on a JEOL ECS-400. ROESY, ^{1}H NMR, ^{13}C NMR, COSY, HMQC, and HMBC spectrum of **1-Pip** were recorded with the following conditions. ROESY spectrum was recorded with relaxation delay of 1.5 s, mixing time of 0.25 s, and receiver gain of 42. COSY spectrum was recorded with relaxation delay of 1.5 s and receiver gain of 50. HMQC spectrum was recorded with x points of 2048, y points of 1024, relaxation delay of 1.5 s,

and receiver gain of 50. HMBC spectrum was recorded with x points of 2048, y points of 1024, relaxation delay of 1.5 s, and receive r gain of 86.

ROESY, ^{1}H NMR, ^{13}C NMR, COSY, HMQC, and HMBC spectrum of **5-Pip** were recorded with the following conditions. ROESY spectrum was recorded with relaxation delay of 1.5 s, mixing time of 0.25 s, and receiver gain of 44. COSY spectrum was recorded with relaxation delay of 1.5 s and receiver gain of 50. HMQC spectrum was recorded with x points of 2048, y points of 1024, relaxation delay of 1.5 s, and receiver gain of 50. HMBC spectrum was recorded with x points of 2048, y points of 1024, relaxation delay of 1.5 s, and receiver gain of 88.

Chemical shifts of ^{1}H NMR, ^{13}C NMR, COSY, HMQC, HMBC, and ROESY spectrum are reported in ppm relative to internal standards (δH, tetramethylsilane 0 ppm; δC, tetramethylsilane 0 ppm). Assignment of ^{1}H NMR was assisted by COSY, HMQC, and HMBC spectrum.

General remarks for computational studies.

All QM calculations were carried out with the Gaussian16 package[8] and all MD simulations were carried out with the Gromacs 2020.4 package[9] and the CHARMM36m/CGenFF force field.[10,11]

Molecular dynamics (MD) simulations.

MD simulations of oligo-NSAs alone were performed using the two different initial structures. A conformation derived from density functional theory (DFT) calculations was used as the initial structure. More specifically, the DFT-optimized structure of acetyl-*N*-ethylalanine pentamer dimethylamide was used as a template and N-substituents of each compound were grafted on the template. When N-substituents were grafted, redundant structures were removed from the template. The substituent-grafted structures were minimized by molecular mechanics calculations using MMFF94s as a force field with fixed backbone atoms (N, N_{α}, N_{β}, C_{α}, C_{β}, and C=O) except for hydrogens. The energy minimization was conducted using Avogadro: an open-source molecular builder and visualization tool. Version 1.1.1. (http://avogadro.cc/).[12] The procedure for preparation of the template structure of acetyl-*N*-ethylalanine pentamer dimethylamide was described in the following section. The initial conformation was solvated with TIP3P water[13] in a rectangular box such that the minimum distance to the edge of the box was 15 Å under periodic boundary conditions. Na and Cl ions were added to imitate a salt solution of concentration 0.15 M. The system was energy-minimized by the steepest descent algorithm (5,000 steps), and heated from 50 K to 298 K during 200 ps, and the simulations were continued by 300 ps with NVT ensemble, where peptoid atoms were held fixed whereas non-peptoid atoms freely moved. Further simulations were performed with NPT ensemble at 298 K for 500 ns without any restraints other

than the LINCS algorithm[14] to constrain bonds involving hydrogen atoms. For each system, the simulation was repeated 5 times with different initial velocities (i.e. 2.5 μs in total for each peptoid initial structure). The time step was set to 2 fs throughout the simulations. A cutoff distance of 12 Å was used for Coulomb and van der Waals interactions. Long-range electrostatic interactions were evaluated by means of the particle mesh Ewald method.[15] A snapshot was saved every 100 ps. For the analysis of each trajectory, we employed the last 400 ns. Representative structures were obtained from clustering of the trajectory. More specifically, clustering analysis was conducted based on the coordinates of five backbone α-carbons of oligo-NSAs using 1 frame per 20 frames from the total 40,010 frames of two series of MD simulations using the different initial structures (5 runs each) with an ensemble clustering tool implemented with UCSF Chimera.[16,17] Representative structures of top 5 clusters were selected as dominant conformations.

MD simulations of the complexes of MDM2 and oligo-NSAs were performed in a similar manner with the above MD simulations of the oligo-NSA alone. The CHARMM36m force field was used to model the MDM2 in complex with oligo-NSAs.[10] For each simulation, an initial structure of the complex was generated using a conformation of oligo-NSA from the MD simulations and a previously reported crystal structure of MDM2. More specifically, for oligo-NSA, a structure with orientations of N-substituents matching to the orientations of three hot-spot residues of p53 (Phe19, Trp23, Phe26) was selected from the trajectory of the above-described MD simulations of each oligo-NSA alone and used as the initial structure. For MDM2, a structure from a co-crystal structure of MDM2 and p53 (PDB 1YCR) was used as the initial structure. Missing residues in the MDM2 structure were complemented using Modeller.[18] The structure of p53 in the co-crystal structure of MDM2 and p53 (PDB 1YCR) were then replaced with the initial structures of oligo-NSA, and the resulting complex was used as the initial coordinates for the subsequent MD simulations. For the analysis of each trajectory, we employed the last 400 ns. Representative conformations were obtained from clustering of the trajectory. More specifically, clustering analysis was conducted based on the coordinates of five backbone α-carbons of oligo-NSAs using 1 frame per 20 frames from the total 20,005 frames of 5 simulations with an ensemble clustering tool implemented with UCSF Chimera.[16,17] Representative structures of top 5 clusters were selected as dominant binding mode. SASA of each N-substituent on oligo-NSAs in complex with MDM2 was calculated with Gromacs 2020.4 package.[9] Calculated SASA was normalized by SASA calculated from trajectory where MDM2 was removed, and the normalized SASA during simulations were plotted and evaluated.

Preparation of a template structure of acetyl-*N*-ethylalanine pentamer dimethylamide.

The energy landscapes about φ and ψ of acetyl-*N*-methylalanine dimethylamide were generated by combinatorially fixing φ and ψ at every 15° from –180° to 180°. Each conformer was optimized at the B3LYP/6-31G* level using a Self-consistent reaction field (SCRF) model with water as the solvent. The ω angles were fixed to 180° through the calculations. Angles with the lowest energy were determined to be (φ, ψ) = (–120º, 90º). Next, the energy landscapes about χ of acetyl-*N*-ethylalanine dimethylamide were generated by optimizing a conformer with χ angle of –180° to 180° with 10° increment. The calculation started with an initial conformation of (χ, φ, ψ) = (0°, –120°, 90°). Angles with the lowest energy were determined to be χ = –90º or 90º. Finally, conformations of acetyl-*N*-ethylalanine pentamer dimethylamide with dihedral angles (χ, φ, ψ, ω) of (–90°, –120°, 90°, 180°) and (90°, –120°, 90°, 180°) were optimized at the B3LYP/6-31G* level using a SCRF model with water as the solvent.

Supporting Figures & Tables

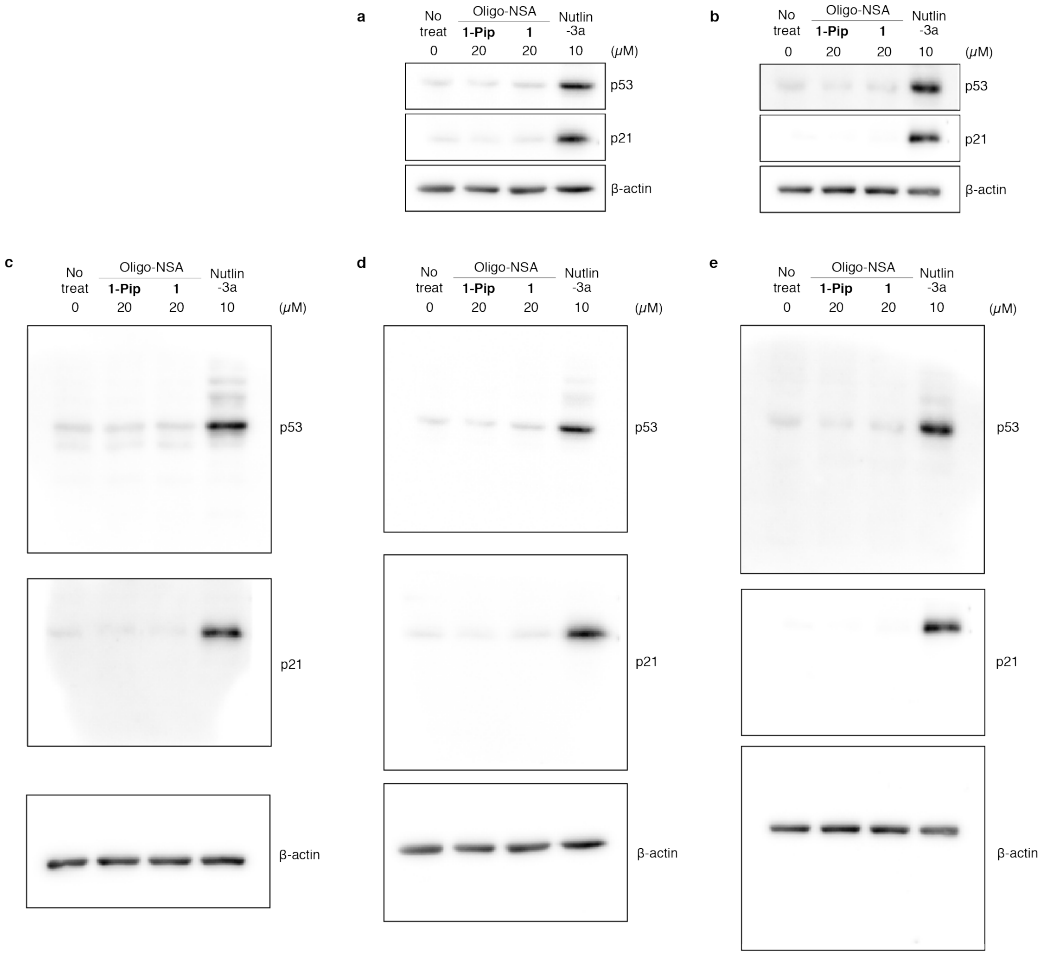

Fig. S1 Intracellular protein levels of p53, p21, and β-actin analyzed by western blotting. SJSA-1 cells were treated with 20 μM **1-Pip** or **1** or 10 μM Nutlin-3a for 8 h. (a, b) Results of two of three independent experiments are shown. Another result is shown in Fig. 2b. (c) Uncropped image of Fig. 2b. (d, e) Uncropped image of Fig. S1a and b.

Table S1 Parameters obtained from the curve fitting (Hill equation: $y = y_{max} - y_{max}/(1 + (IC_{50}/x)^n)$) of the data in a competitive FP assay of **1-Pip** and **1**. Inhibitory curves are shown in Fig. 2c.

Compound	y_{max}	IC_{50} (μM)	n
1-Pip	39.3 ± 0.3	12 ± 1	0.96 ± 0.05
1	41.2 ± 0.4	18 ± 1	1.06 ± 0.05

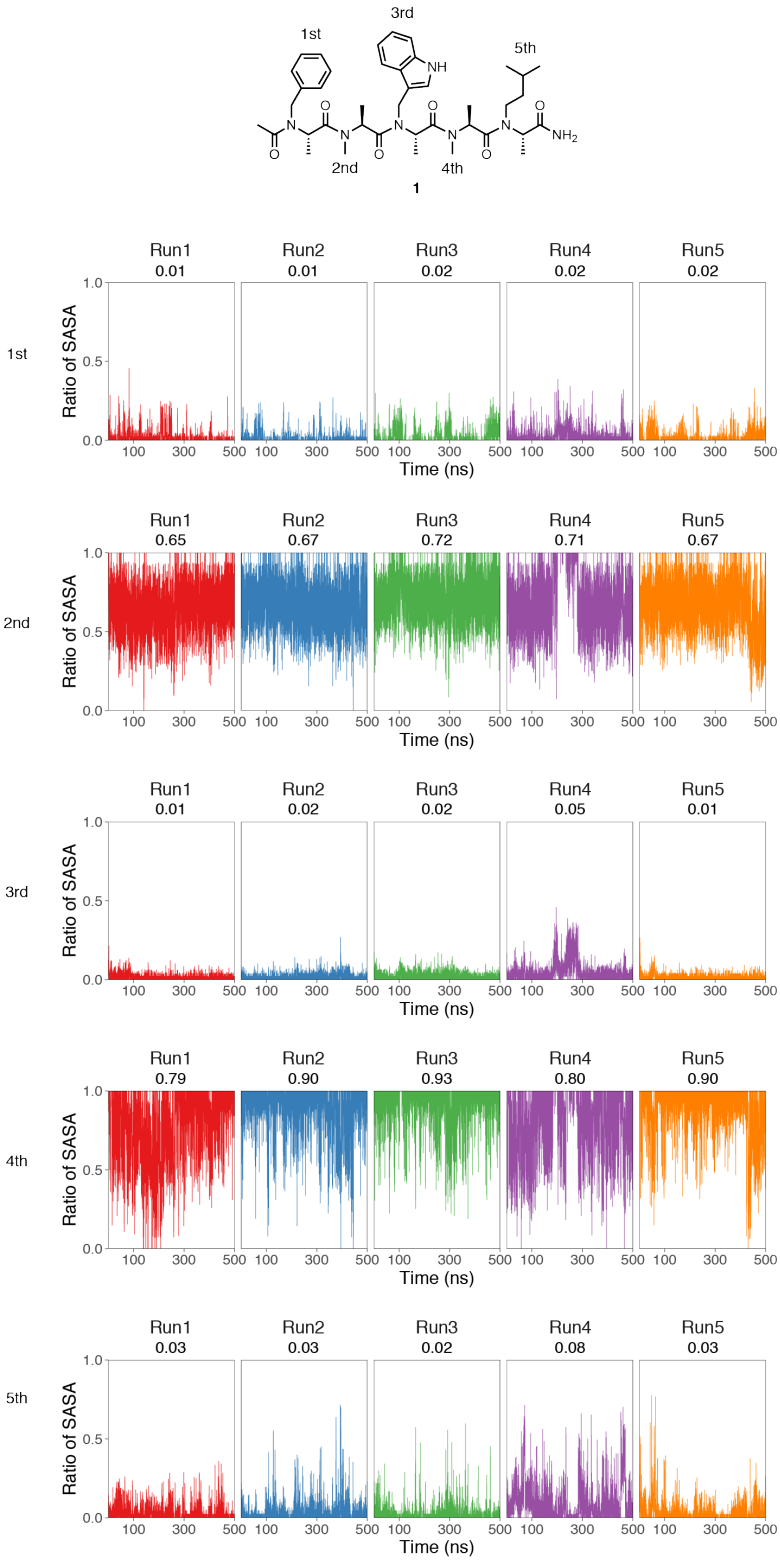

Fig. S2 Ratio of SASA to the whole surface area of each N-substituent during each MD run is plotted. The average during MD run is shown above each plot.

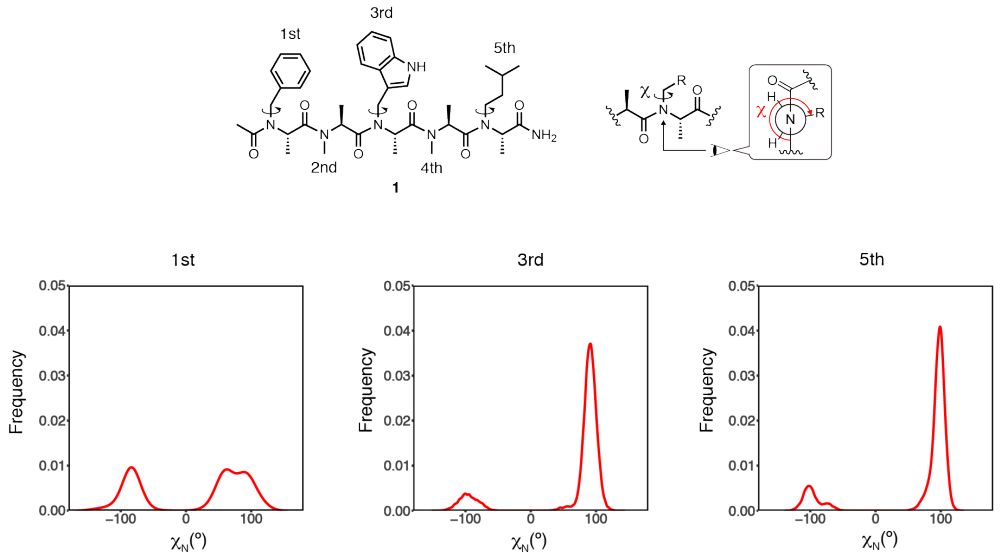

Fig. S3 Distributions of χ angles of **1** during MD simulations. The distributions of 1st, 3rd and 5th residues are shown.

Table S2 Chemical structures of substituents at R_1, R_3, and R_5 and K_i values of compounds **S1**–**S7**.

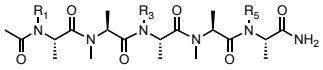

Compound	R_1	R_3	R_5	K_i (μM)[a]
S1				22.3 ± 1.9
S2				6.0 ± 1.2
S3				24.9 ± 3.9
S4		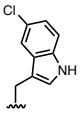		2.7 ± 0.2
S5		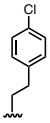		1.9 ± 0.6
S6		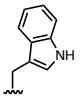		10.6 ± 3.2
S7				23.8 ± 1.3

[a]The K_i values were determined by a competitive fluorescence polarization assay.

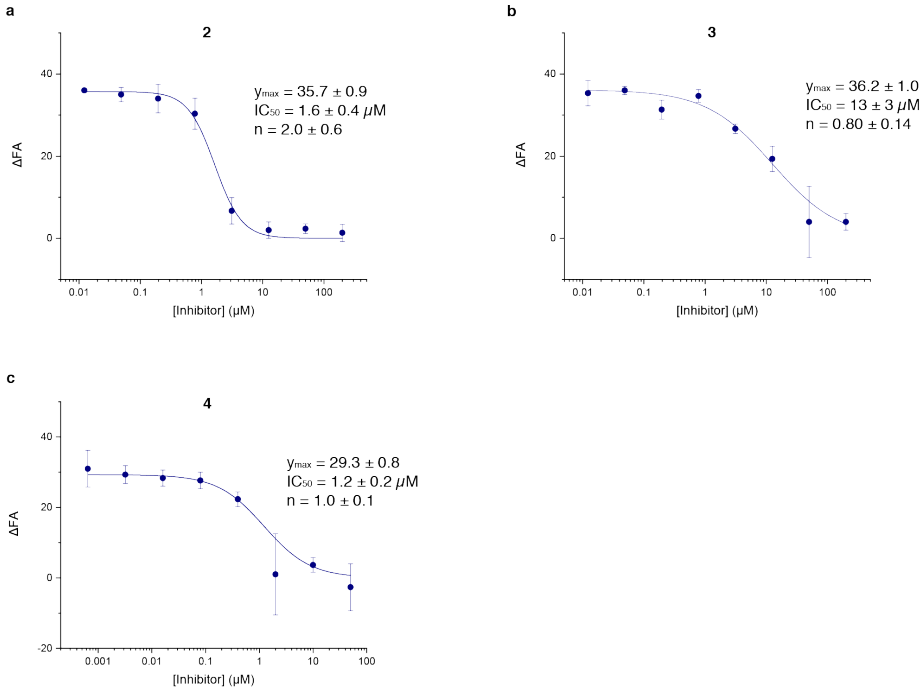

Fig. S4 Inhibitory curves of **2**–**4** against the interaction between fluorescently labeled PMI peptide and MDM2 generated from a competitive FP assay. Error bars represent standard deviations of triplicates. Parameters obtained from the curve fitting (Hill equation: $y = y_{max} - y_{max}/(1 + (IC_{50}/x)^n)$) of the acquired data are shown in each graph.

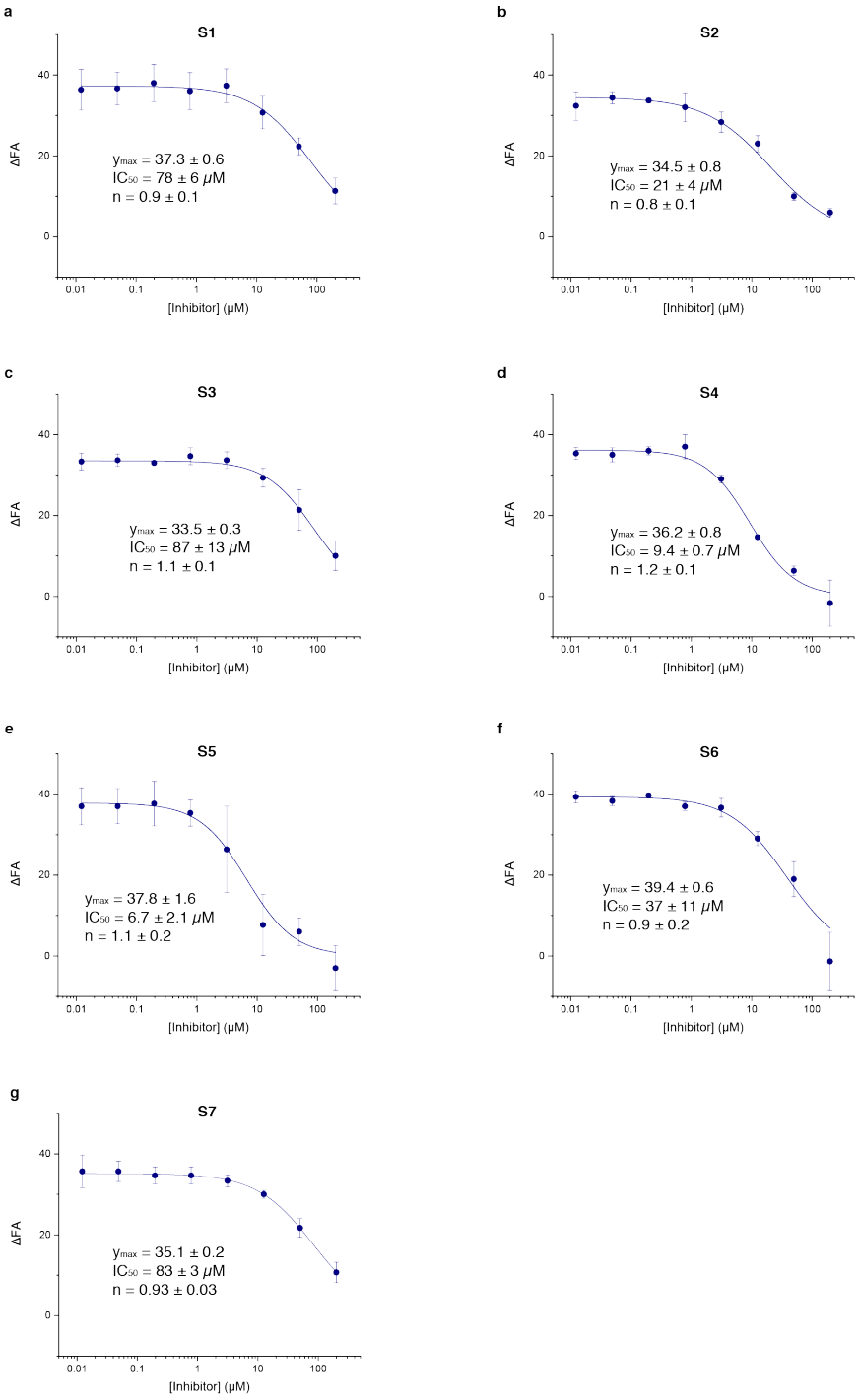

Fig. S5. Inhibitory curves of **S1**–**S7** against the interaction between fluorescently labeled PMI peptide and MDM2 generated from a competitive FP assay. Error bars represent standard deviations of triplicates. Parameters obtained from the curve fitting (Hill equation: $y = y_{max} - y_{max}/(1 + (IC_{50}/x)^n)$) of the acquired data are shown in each graph.

Table S3 Chemical structures of substituents at R_2 and R_4, and P_e values of compound **4**–**9** determined by PAMPA.

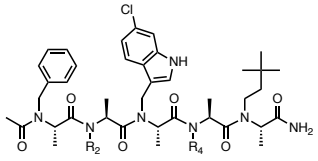

Compound	R_2, R_4	P_e ($\times 10^{-6}$ cm/s)
4	(Me)	0.14 ± 0.03
5	(Et)	0.34 ± 0.02
6	(*n*-Pr)	n.d.[a]
7	(*n*-Bu)	n.d.[a]
8	(Moe)	0.22 ± 0.07
9	(Hoe)	0.14 ± 0.05

[a]Not determined due to the low water solubility in aqueous solution.

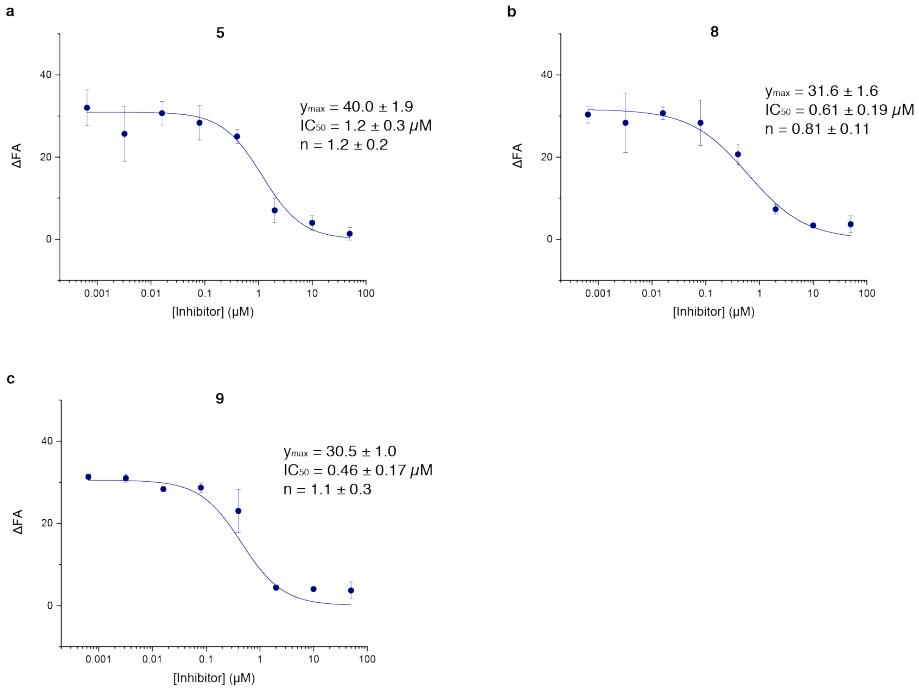

Fig. S6 Inhibitory curves of **5**, **8**, and **9** against the interaction between fluorescently labeled PMI peptide and MDM2 generated from a competitive FP assay. Error bars represent standard deviations of triplicates. Parameters obtained from the curve fitting (Hill equation: $y = y_{max} - y_{max}/(1 + (IC_{50}/x)^n)$) of the acquired data are shown in each graph.

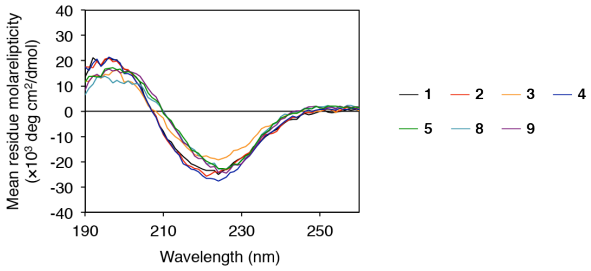

Fig. S7 CD spectra of **1**–**5**, **8**, and **9**. CD spectra were recorded at 25°C with 50 μM solution of each oligomer in 20 mM phosphate buffer (pH 7.4) containing 5% methanol. The Y-axis was normalized to molar ellipticity per residue.

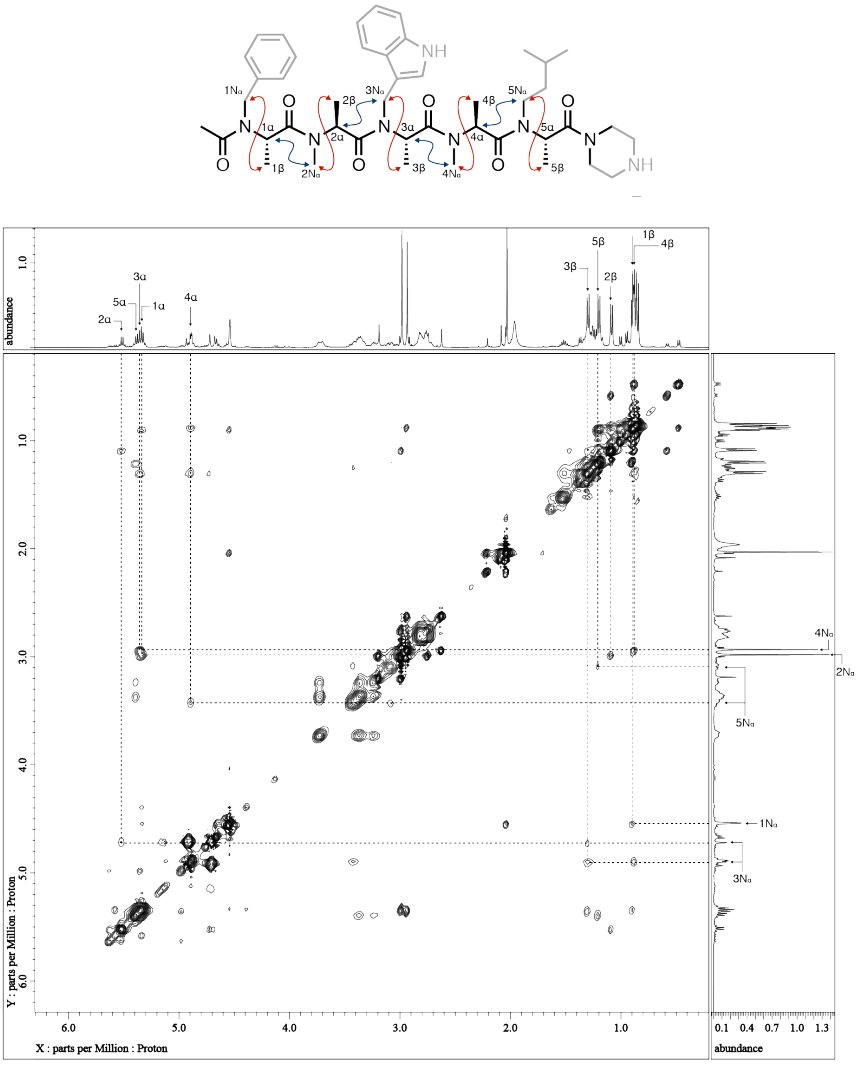

Fig. S8 ROESY spectrum of oligo-NSA **1-Pip**. Spectrum was recorded in $CDCl_3$ at 25°C. NOE peaks that support rotational restriction about backbone dihedral angles, φ and ψ, are shown with dashed lines in the spectrum. Protons that are suggested in proximity are shown with red and blue arrows in the chemical structure.

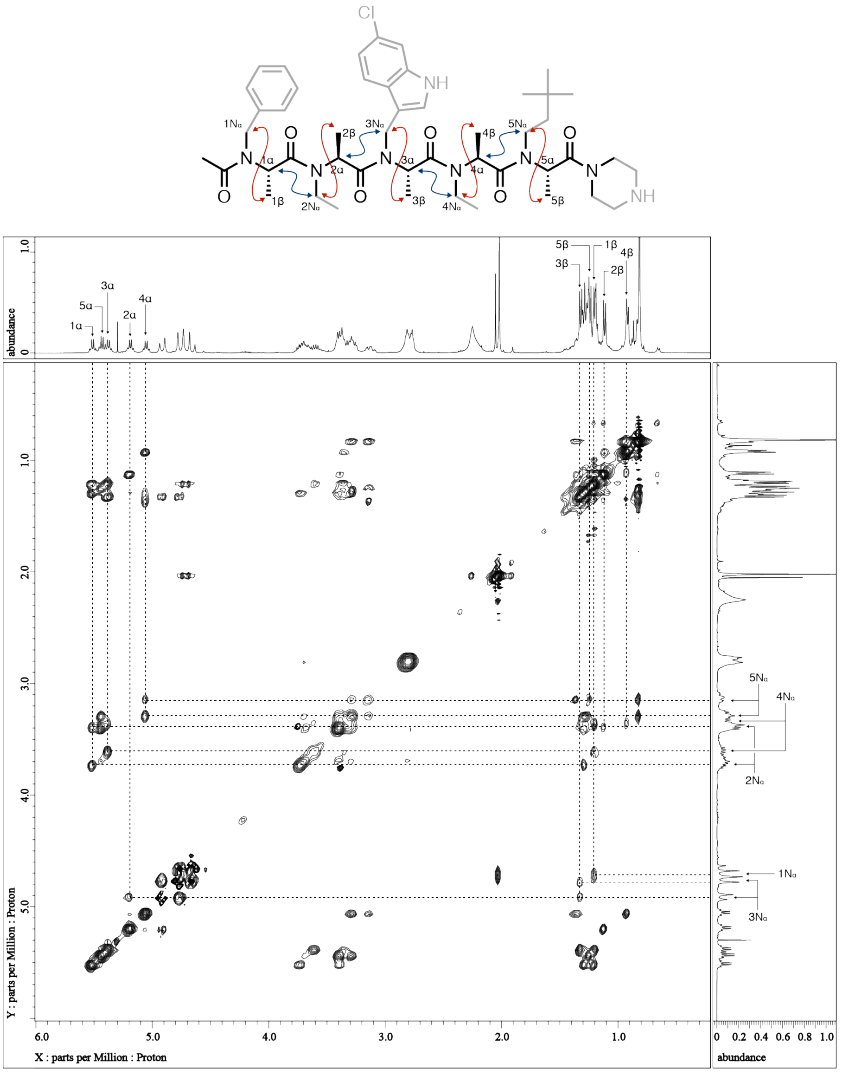

Fig. S9 ROESY spectrum of oligo-NSA **5-Pip**. Spectrum was recorded in $CDCl_3$ at 25°C. NOE peaks that support rotational restriction about backbone dihedral angles, φ and ψ, are shown with dashed lines in the spectrum. Protons that are suggested in proximity are shown with red and blue arrows in the chemical structure.

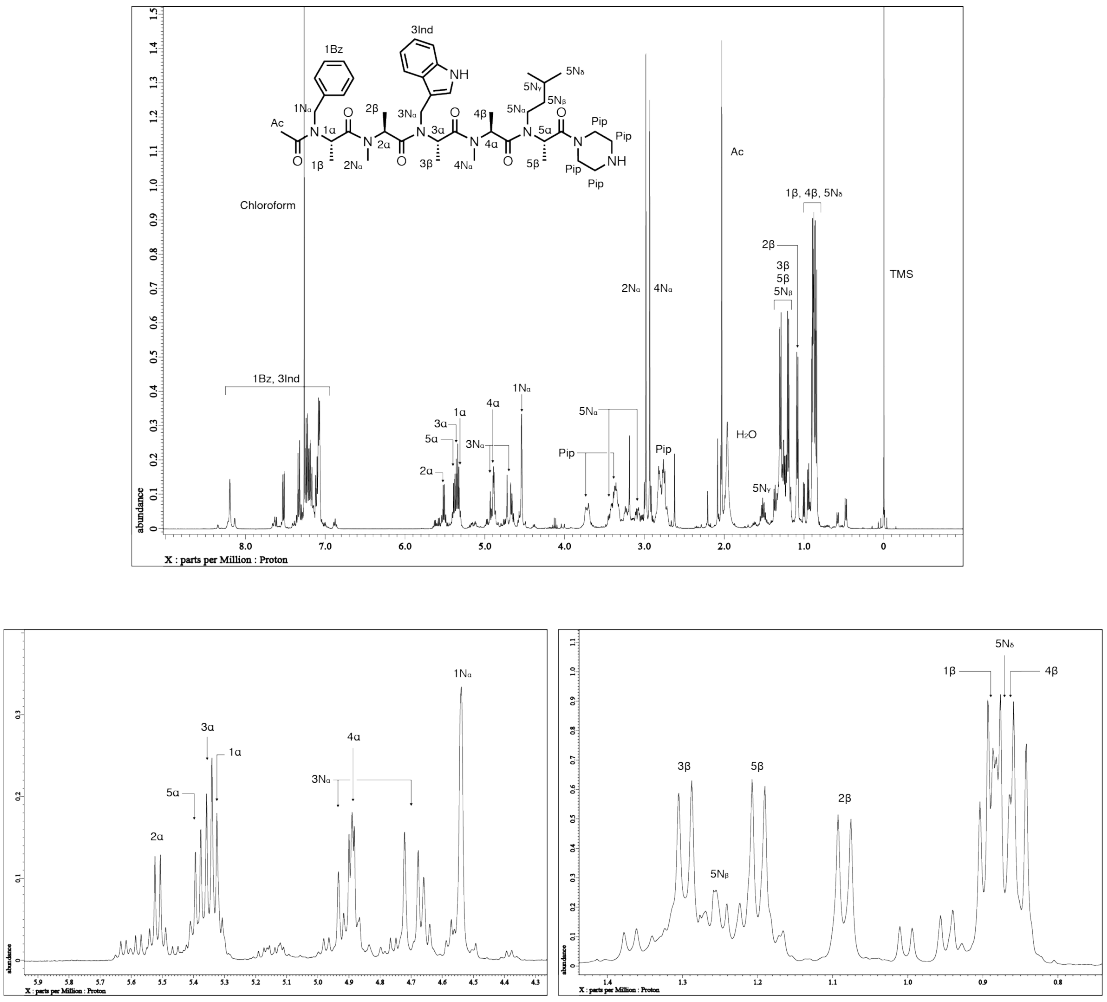

Fig. S10 ^{1}H NMR spectrum of **1-Pip**. Spectrum was recorded in $CDCl_3$ at 25°C. Peaks were assigned with the aid of COSY, ^{13}C NMR, HMQC, and HMBC spectra.

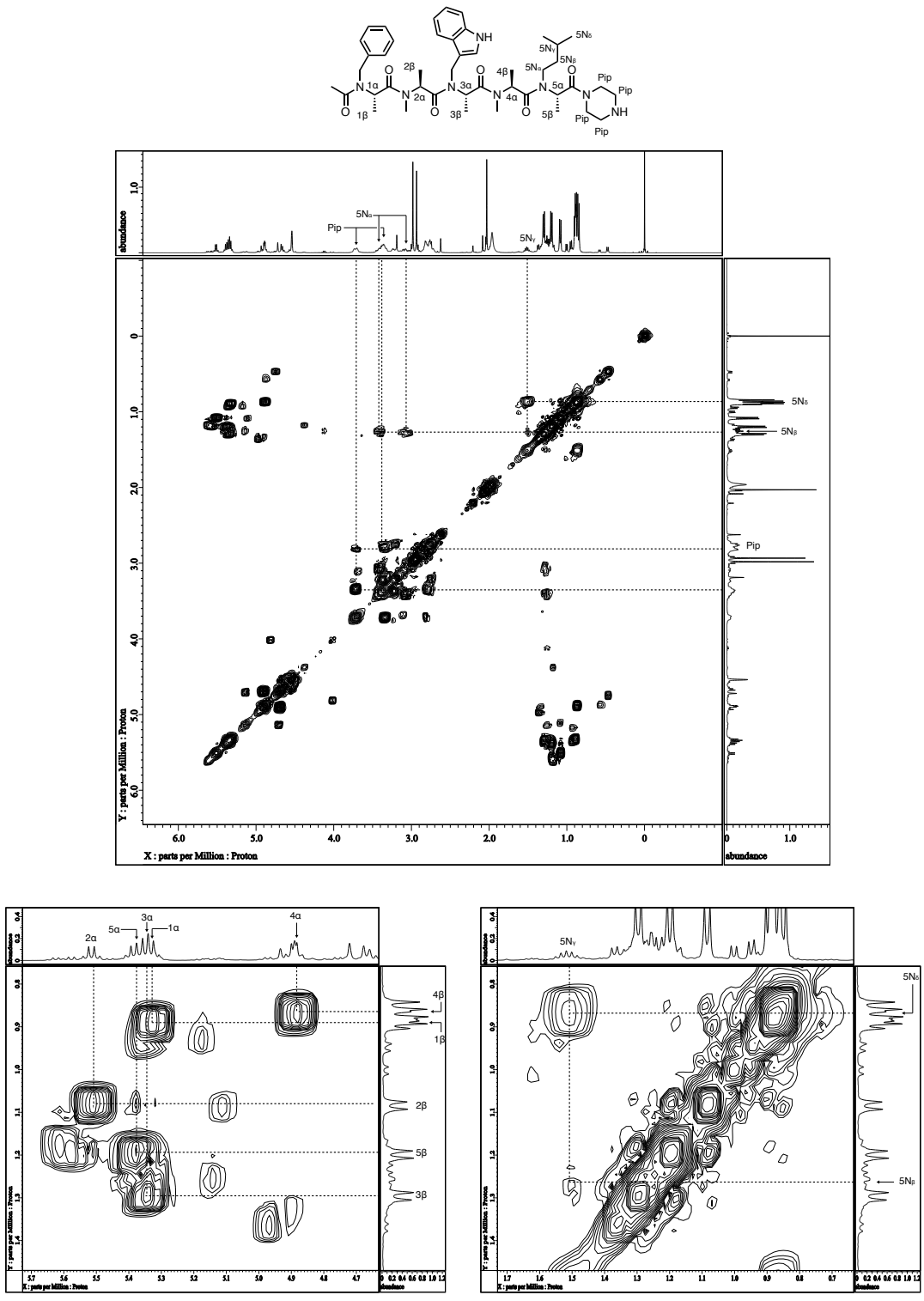

Fig. S11 COSY spectrum of **1-Pip**. Spectrum was recorded in $CDCl_3$ at 25°C. Cross peaks that support assignment of ^1H NMR are shown with dashed lines.

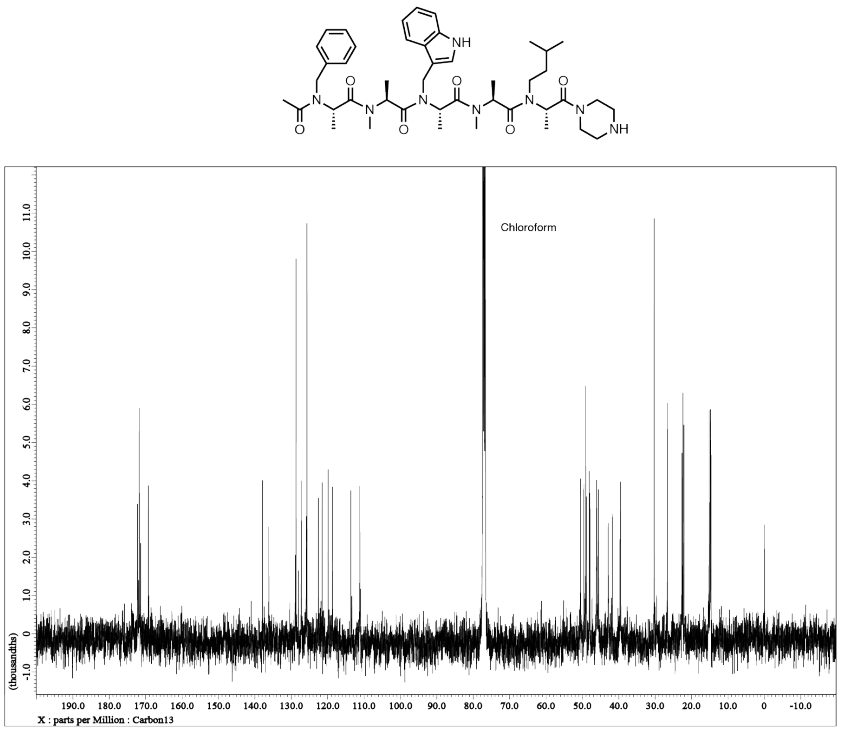

Fig. S12 ^{13}C NMR spectrum of **1-Pip**. Spectrum was recorded in $CDCl_3$ at 25°C.

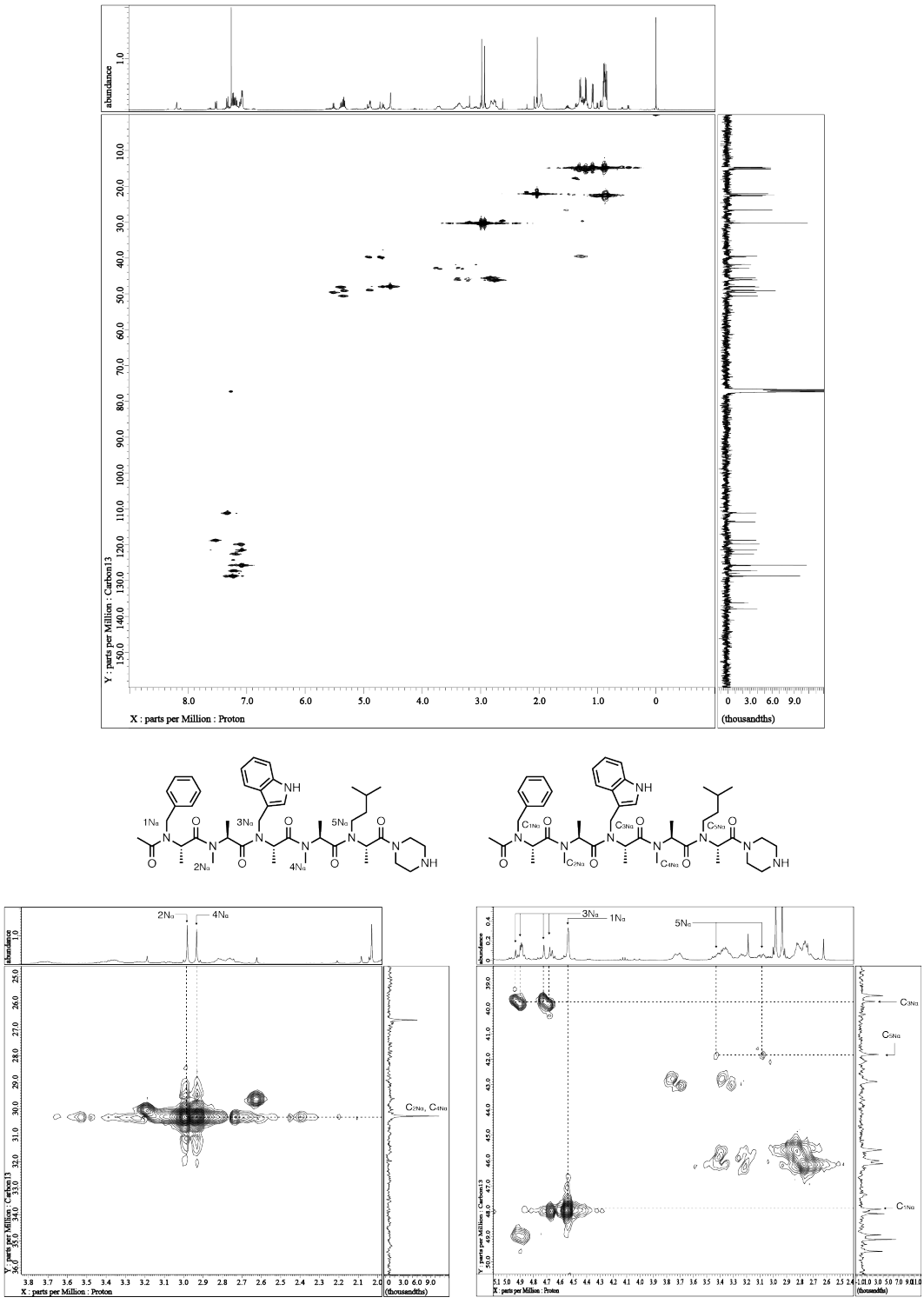

Fig. S13 HMQC spectrum of **1-Pip**. Spectrum was recorded in $CDCl_3$ at 25°C. Cross peaks that support assignment of ^{1}H NMR are shown with dashed lines.

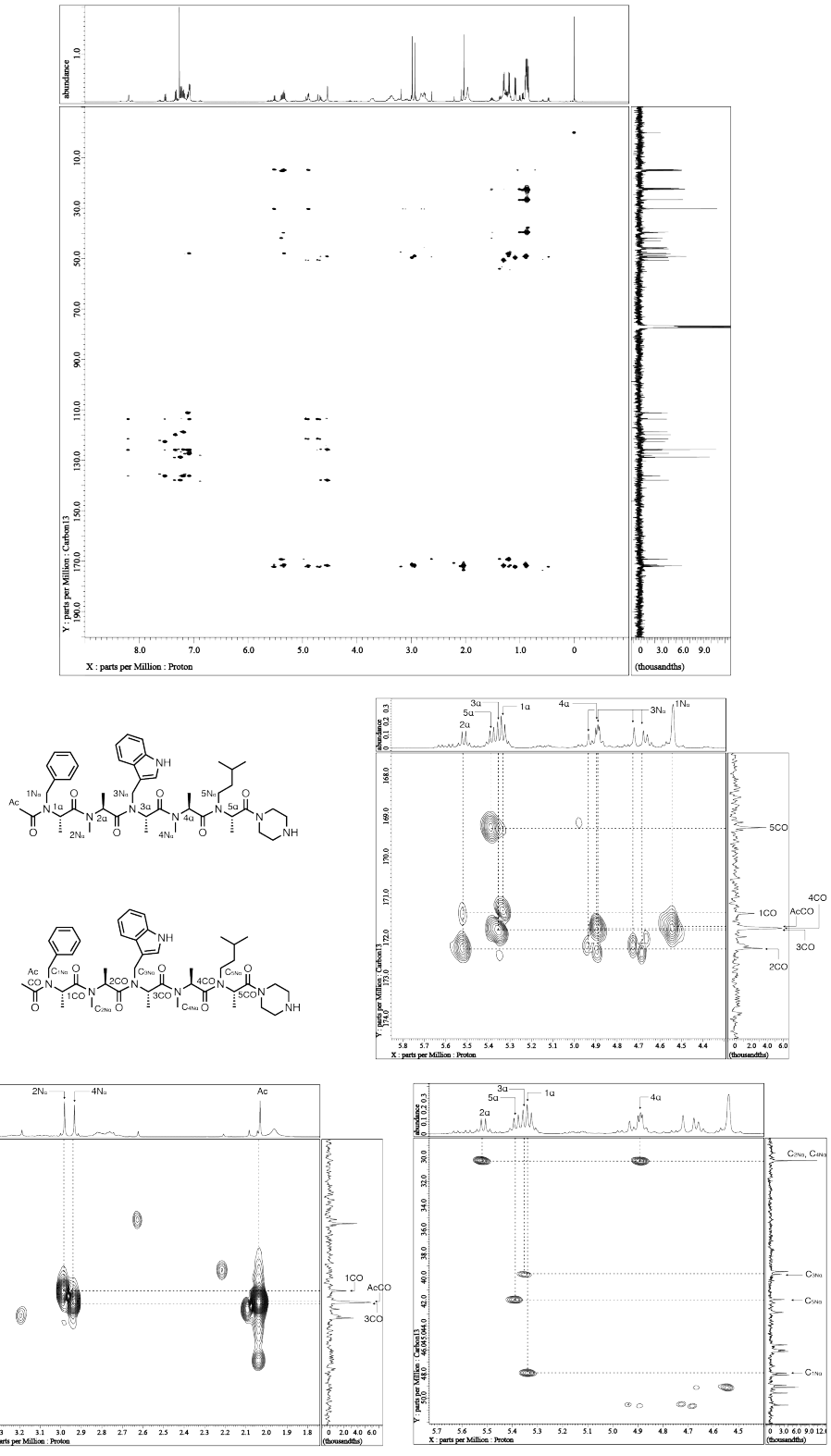

Fig. S14. HMBC spectrum of **1-Pip**. Spectrum was recorded in $CDCl_3$ at 25°C. Cross peaks that support assignment of ^{1}H NMR are shown with dashed lines.

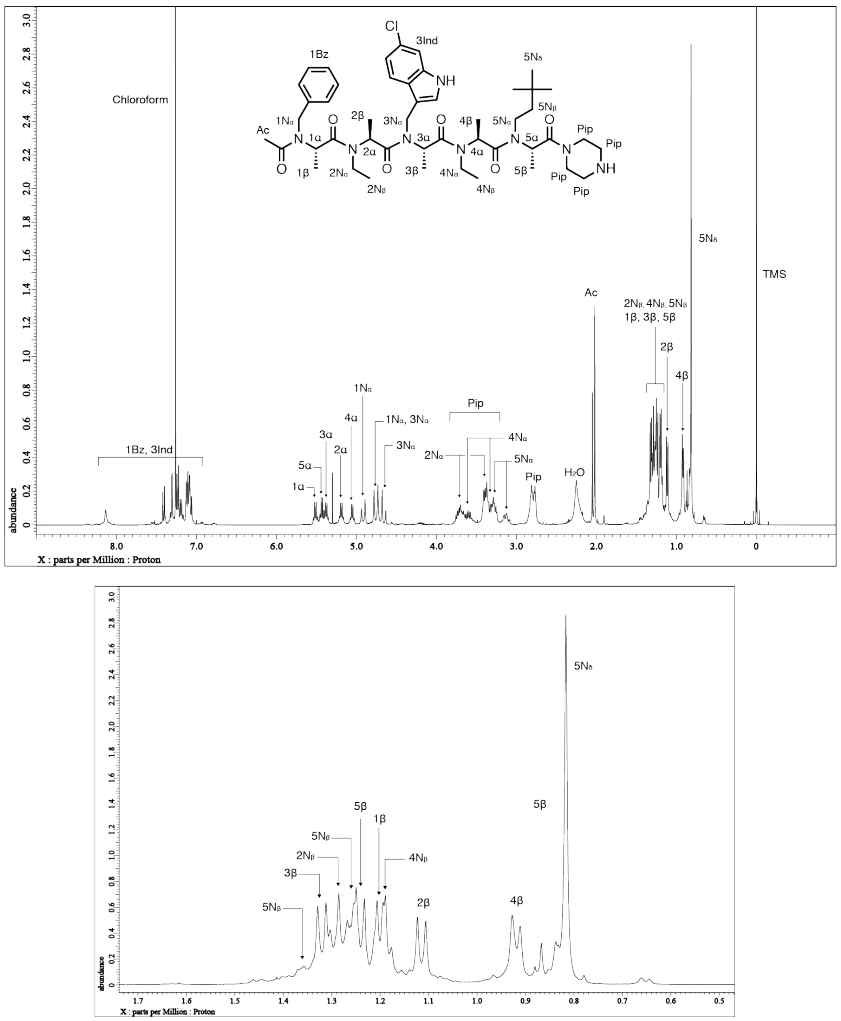

Fig. S15 ^{1}H NMR spectrum of **5-Pip**. Spectrum was recorded in $CDCl_3$ at 25°C. Peaks were assigned with the aid of COSY, ^{13}C NMR, HMQC, and HMBC spectra.

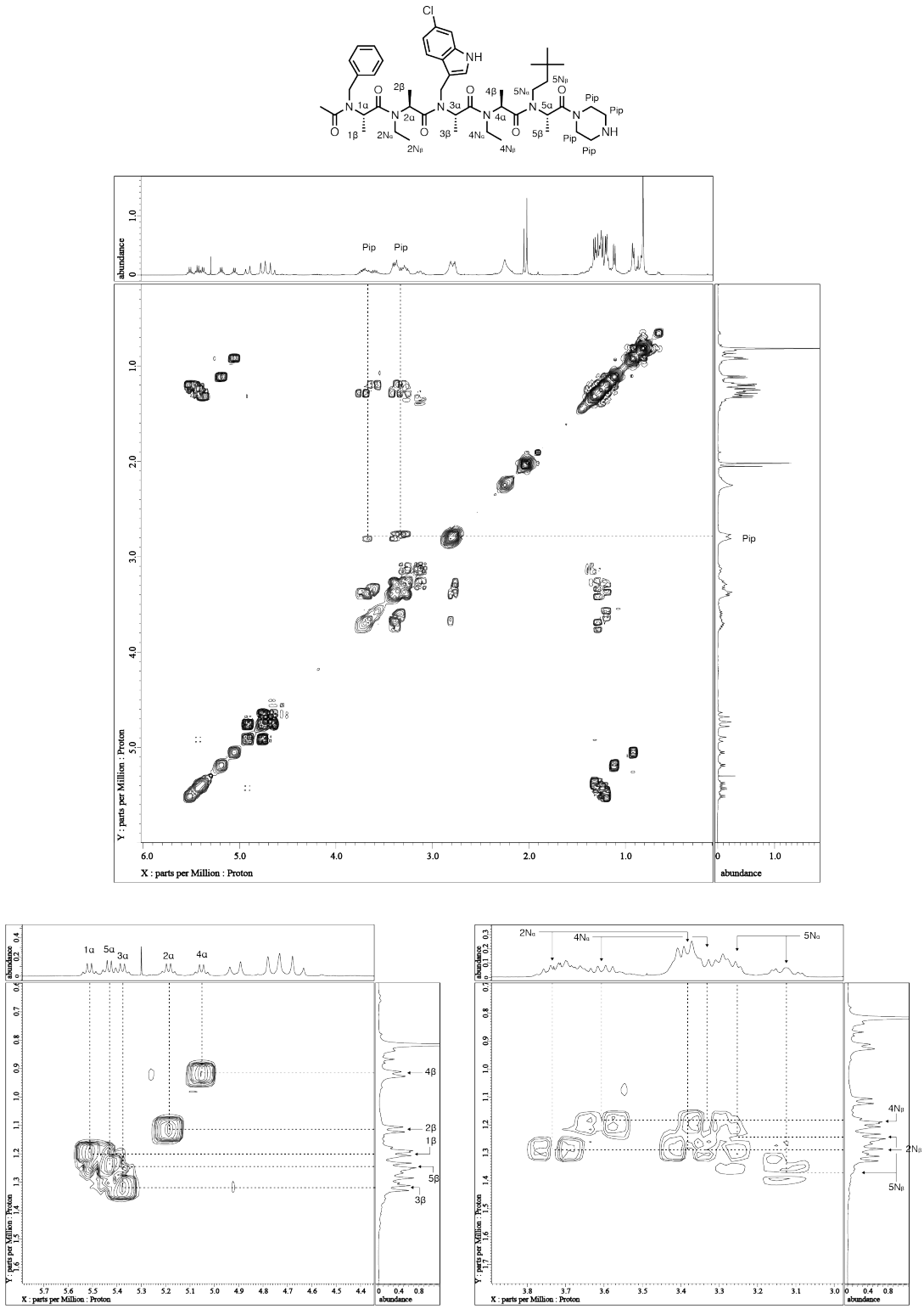

Fig. S16 COSY spectrum of **5-Pip**. Spectrum was recorded in $CDCl_3$ at 25°C. Cross peaks that support assignment of ^1H NMR are shown with dashed lines.

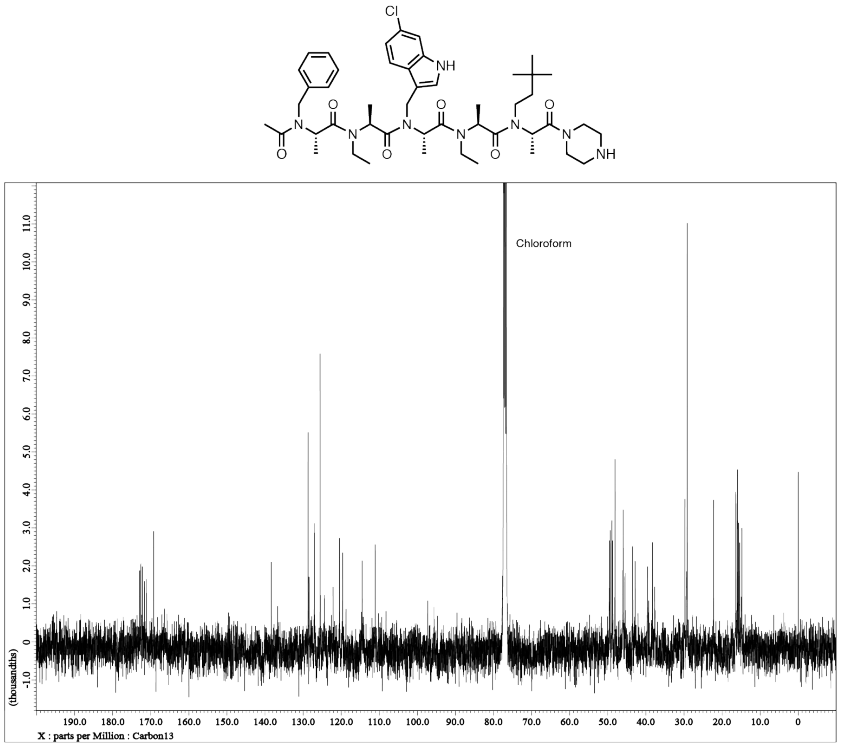

Fig. S17 ^{13}C spectrum of **5-Pip**. Spectrum was recorded in $CDCl_3$ at 25°C.

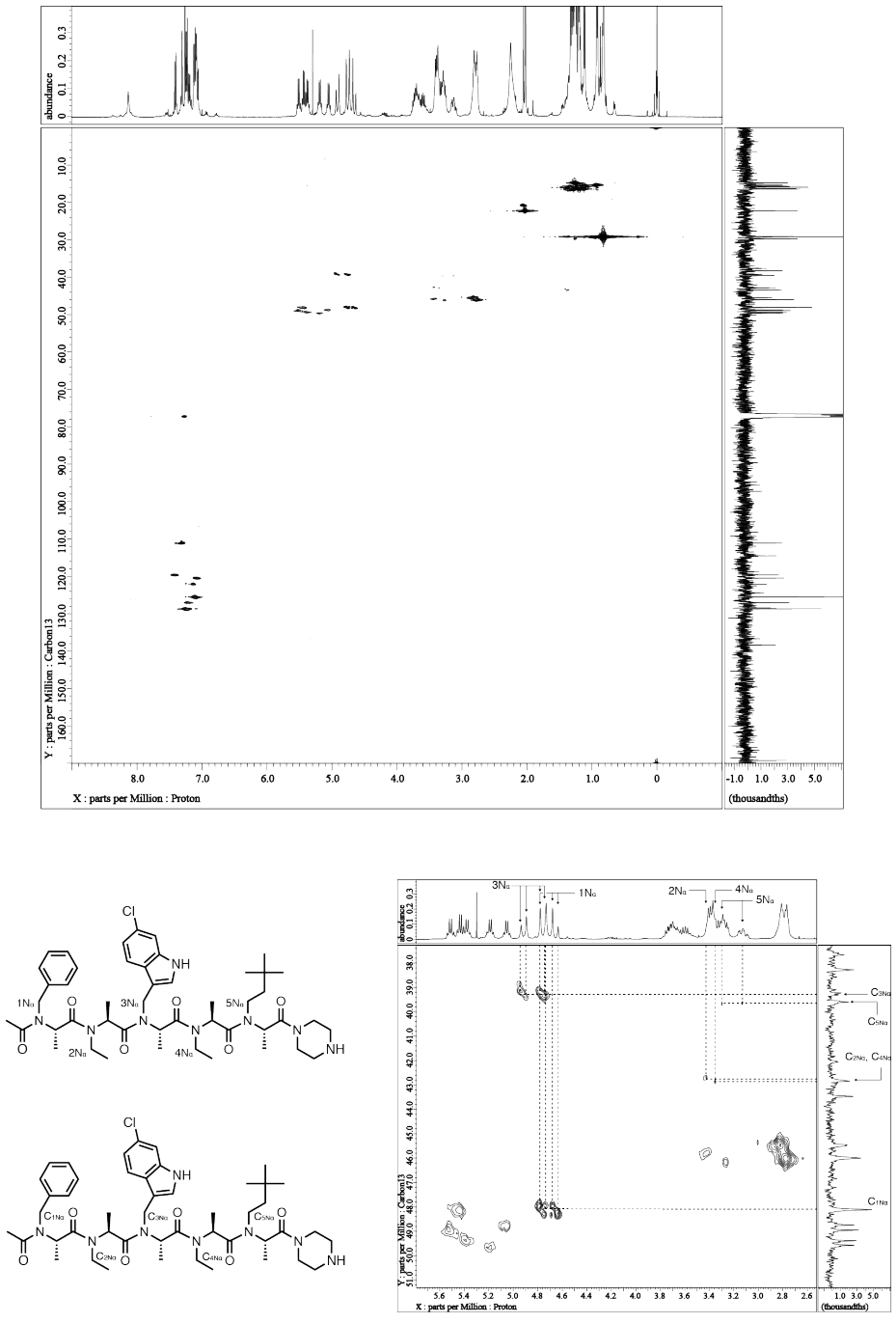

Fig. S18 HMQC spectrum of **5-Pip**. Spectrum was recorded in $CDCl_3$ at 25°C. Cross peaks that support assignment of ^1H NMR are shown with dashed lines.

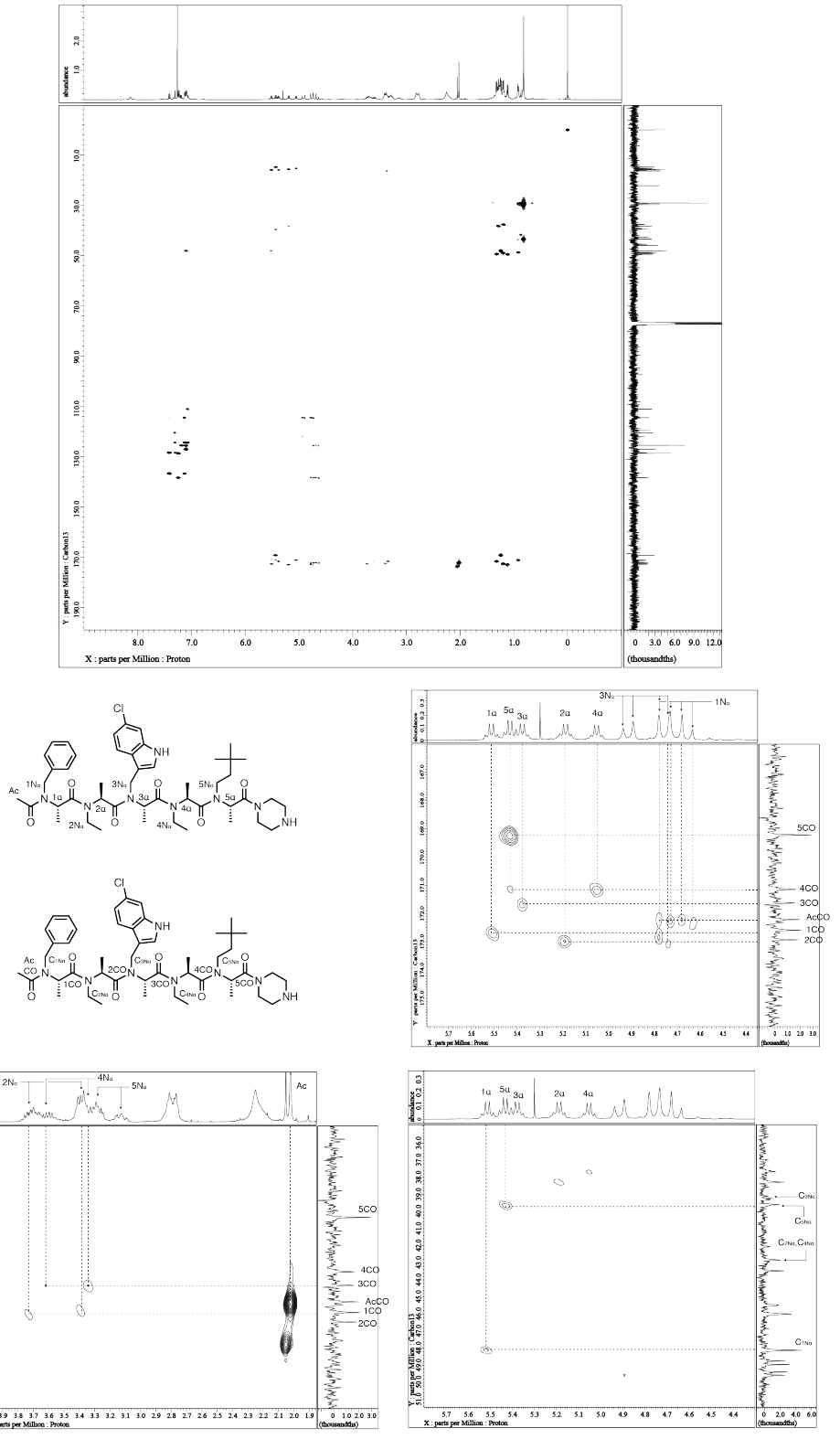

Fig. S19 HMBC spectrum of **5-Pip**. Spectrum was recorded in $CDCl_3$ at 25°C. Cross peaks that support assignment of ^{1}H NMR are shown with dashed lines.

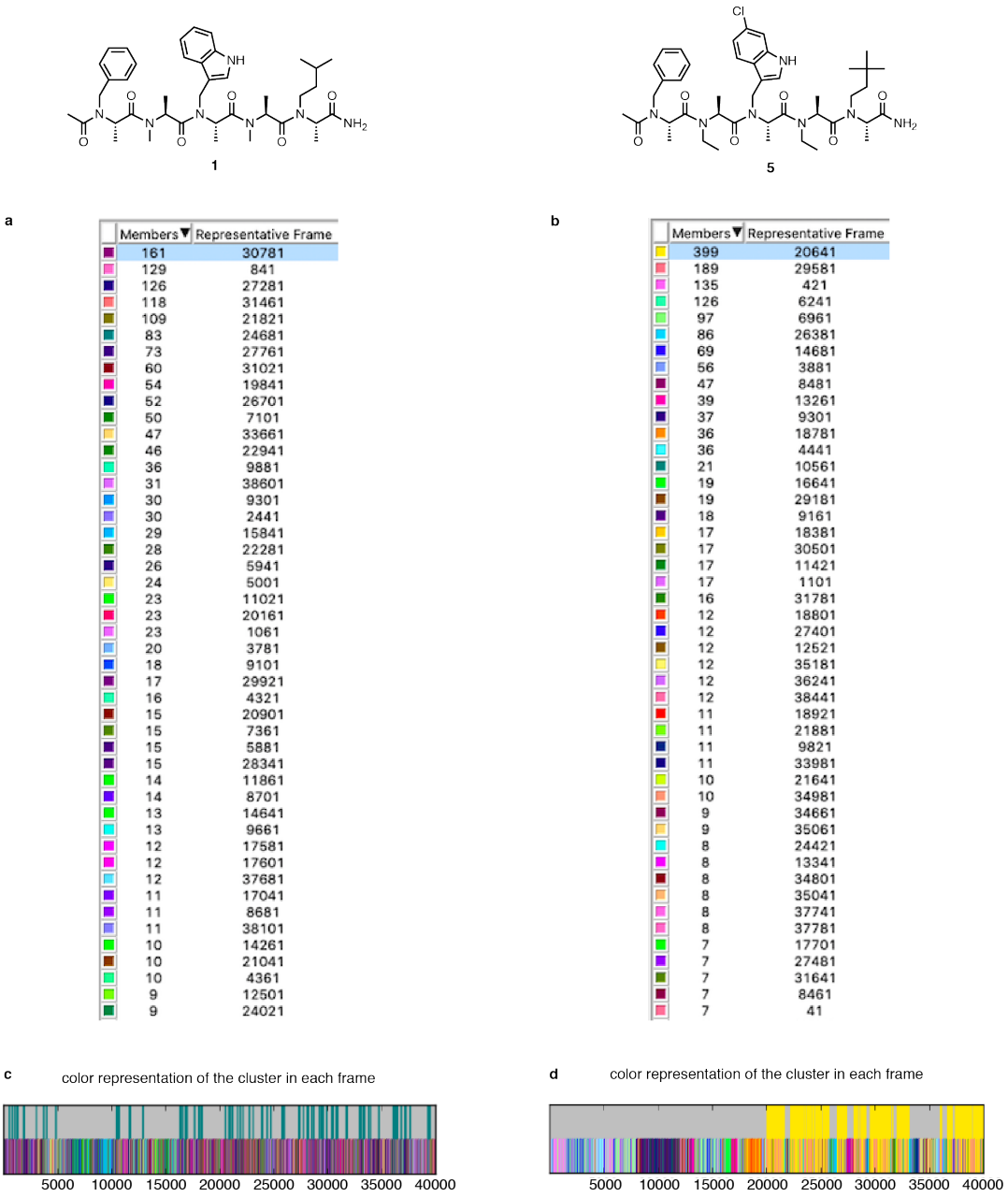

Fig. S20 Clustering results of the MD simulations of oligo-NSA **1** and **5**. Frames from ten runs were combined and the total frames were subjected to the clustering. (a, b) The generated clusters of **1** and **5** and the number of members classified to each cluster. The number of a representative frame is also shown for each cluster. Conformers corresponding to the representative frames of top 5 clusters are overlaid in Fig. 5d and e. (c, d) Each frame was colored using the color of the cluster shown in (a) and (b).

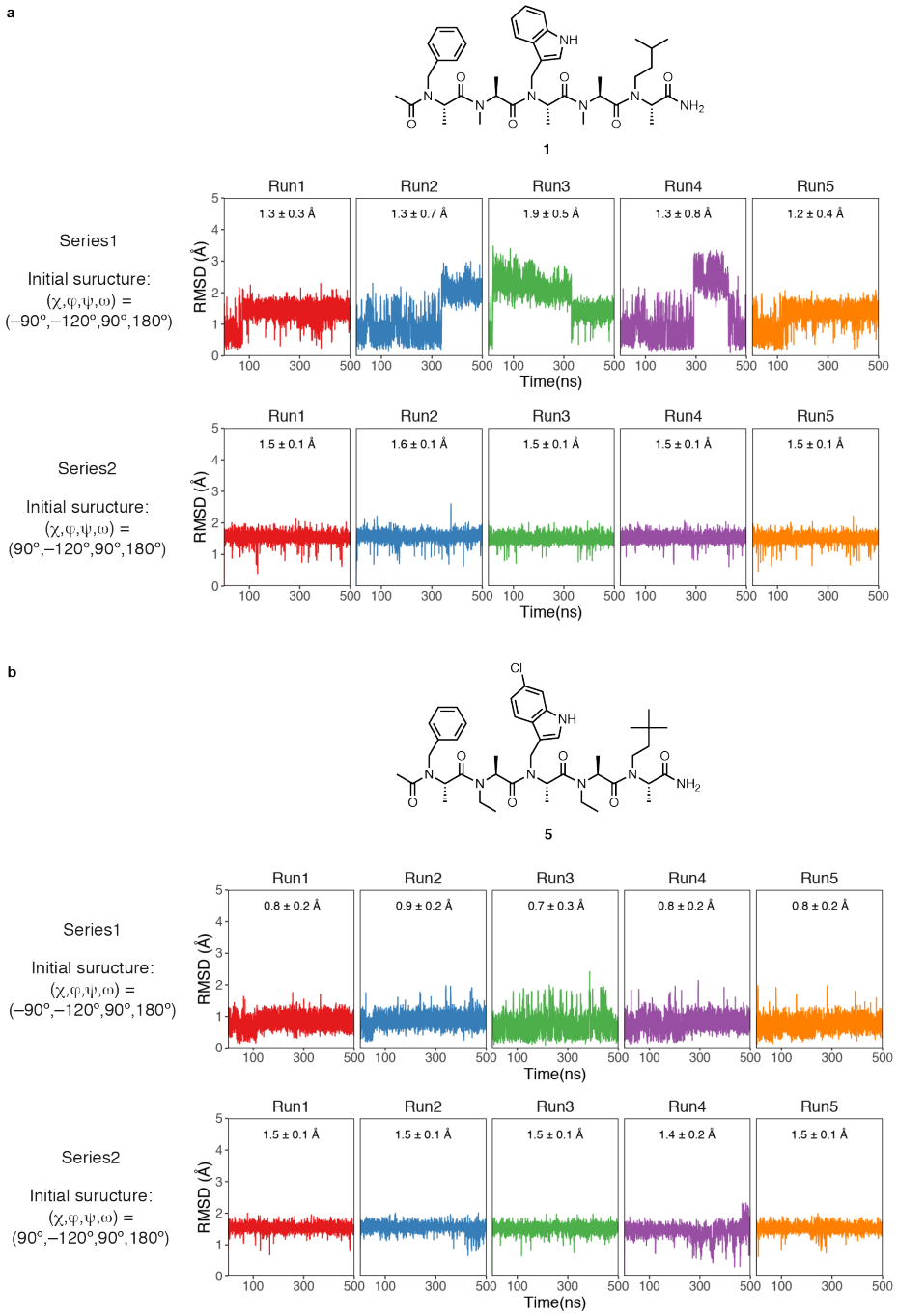

Fig. S21 RMSD values of α-carbons of oligo-NSA **1** and **5** from the initial structures during each MD run are plotted.

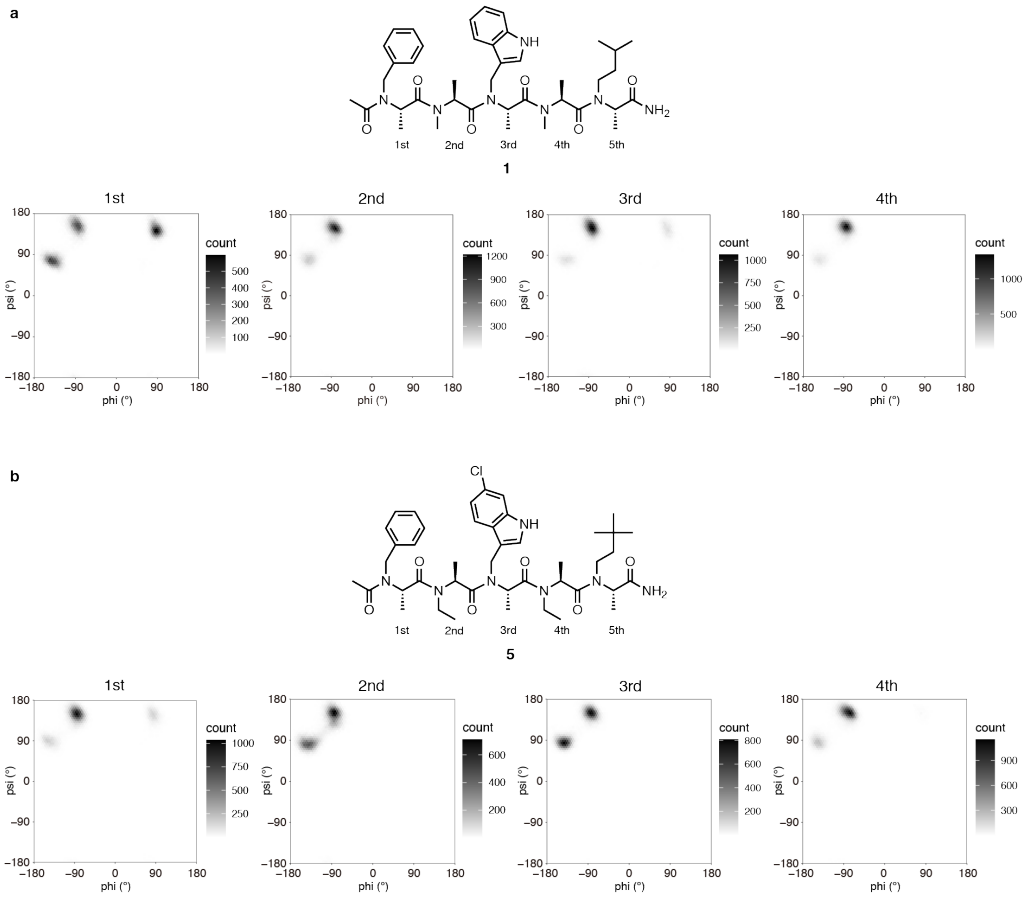

Fig. S22 Distributions of φ and ψ angles of **1** and **5** during MD simulations. The distribution of 1st–4th residues are shown. The distributions of 5th residues are not shown because C terminal amide is not substituted, and 5th residues do not experience rotational restriction of φ and ψ angles by pseudo-1,3-allylic strains.

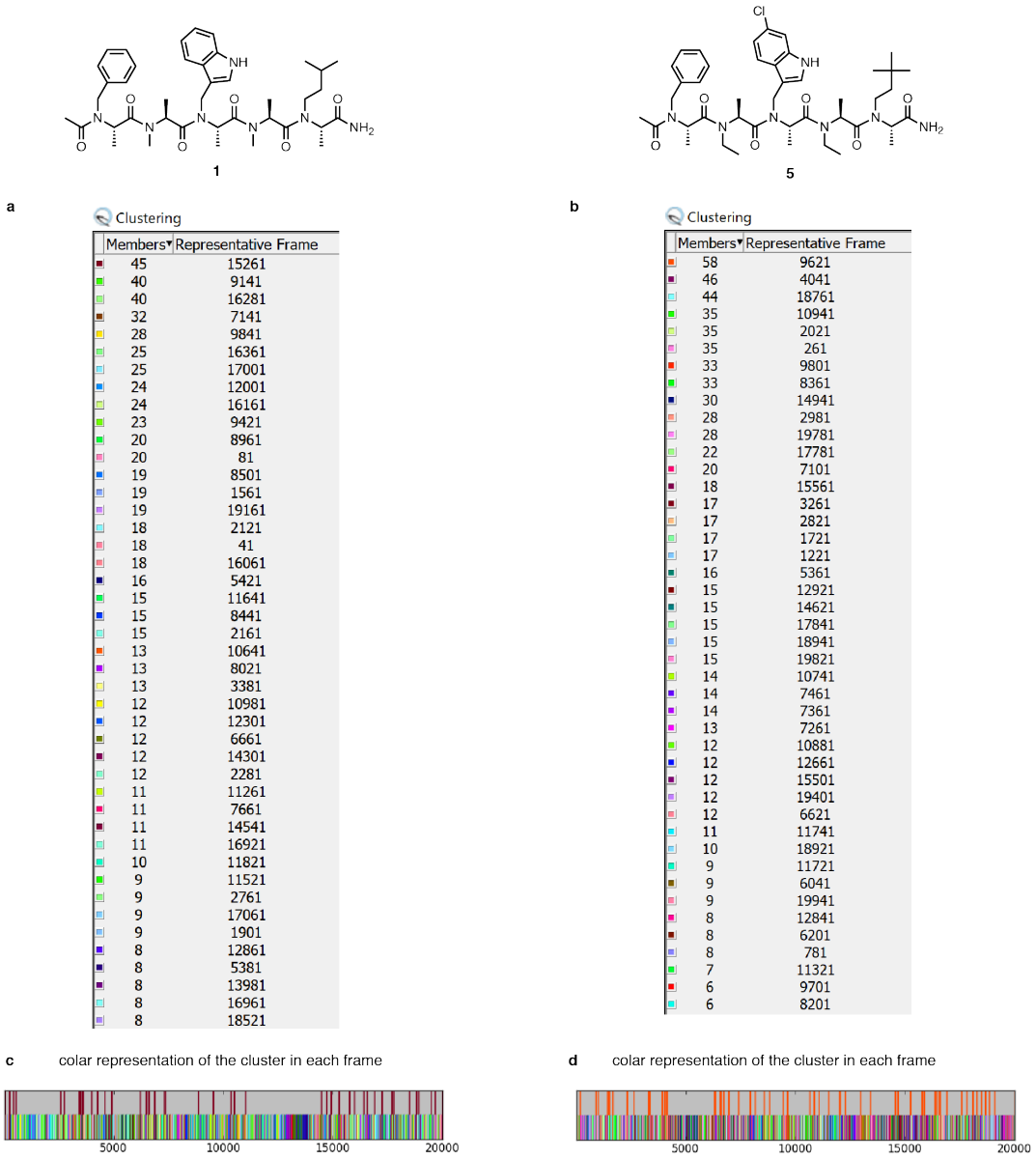

Fig. S23 Clustering results of the MD simulations of oligo-NSA **1** and **5** in complex with MDM2. Frames from five runs were combined and the total frames were subjected to the clustering. (a, b) The generated clusters and the number of members classified to each cluster. The number of a representative frame is also shown for each cluster. (c, d) Each frame was colored using the color of the cluster shown in (a) and (b).

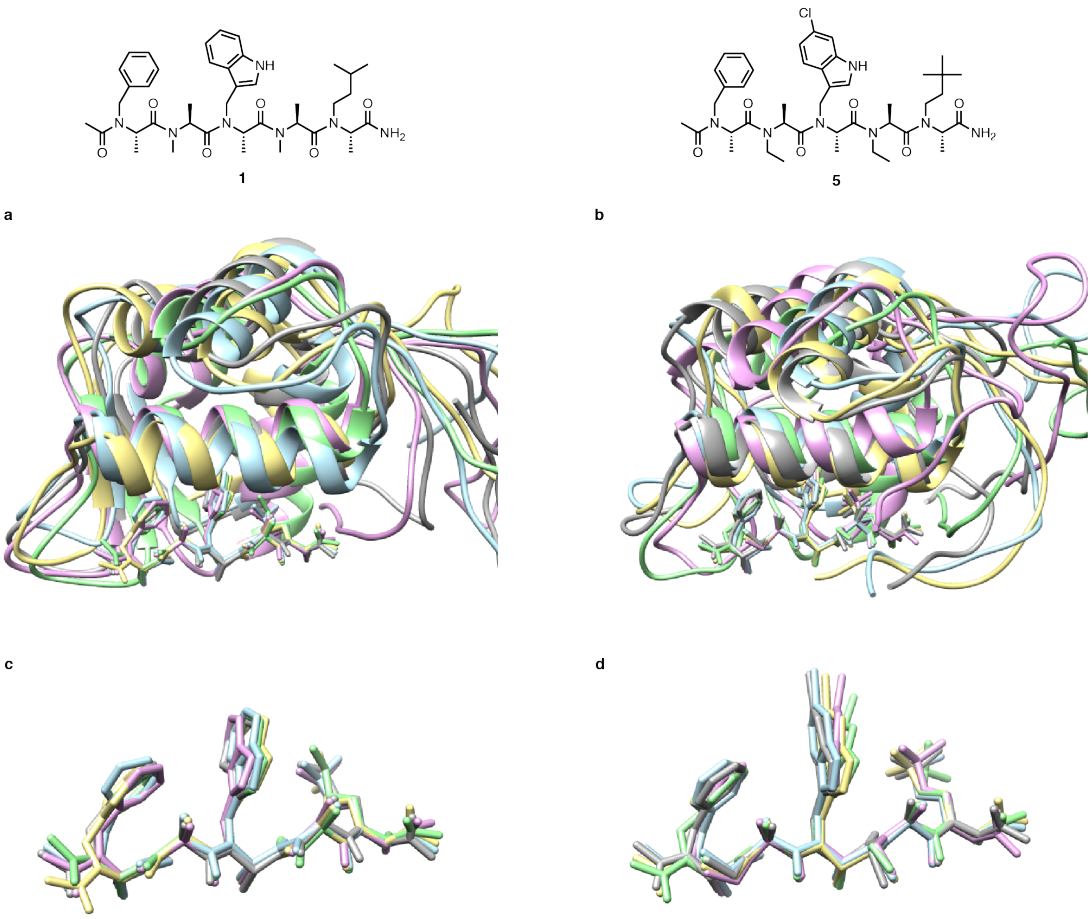

Fig. S24 Clustering results of MD simulations of oligo-NSA **1** and **5** in complex with MDM2. (a, b) Structures corresponding to the representative frames of top 5 clusters are overlaid. (c, d) The structures of oligo-NSA **1** and **5** in (a) and (b) were extracted.

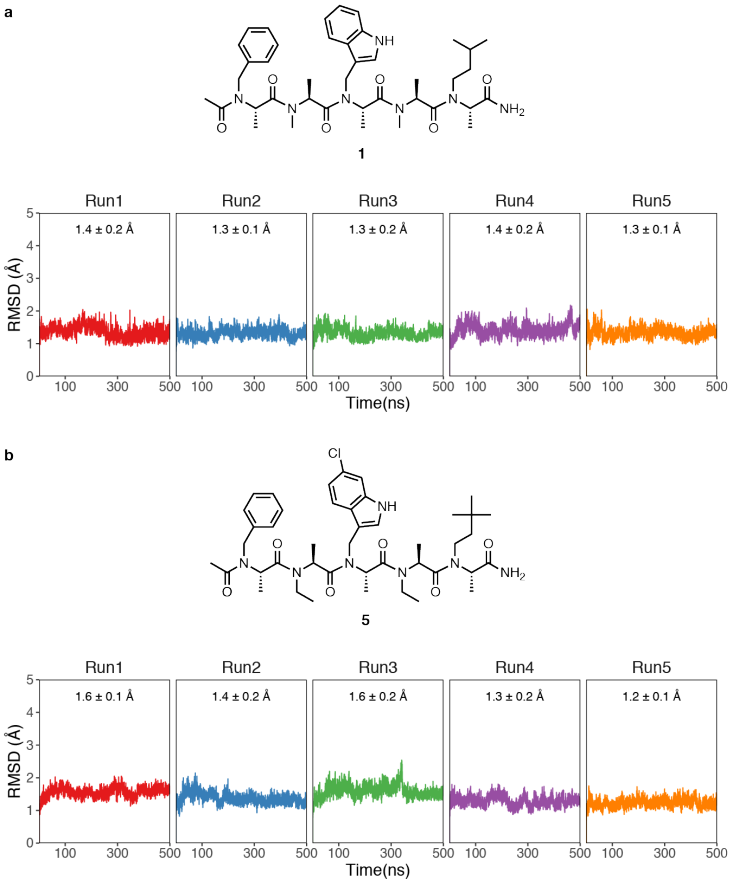

Fig. S25 RMSD values of α-carbons of oligo-NSA **1** and MDM2 (a) or **5** and MDM2 (b) from the initial structures during each MD run are plotted. The results show that the MD simulations have reached well-equilibrated states and valid for further analysis.

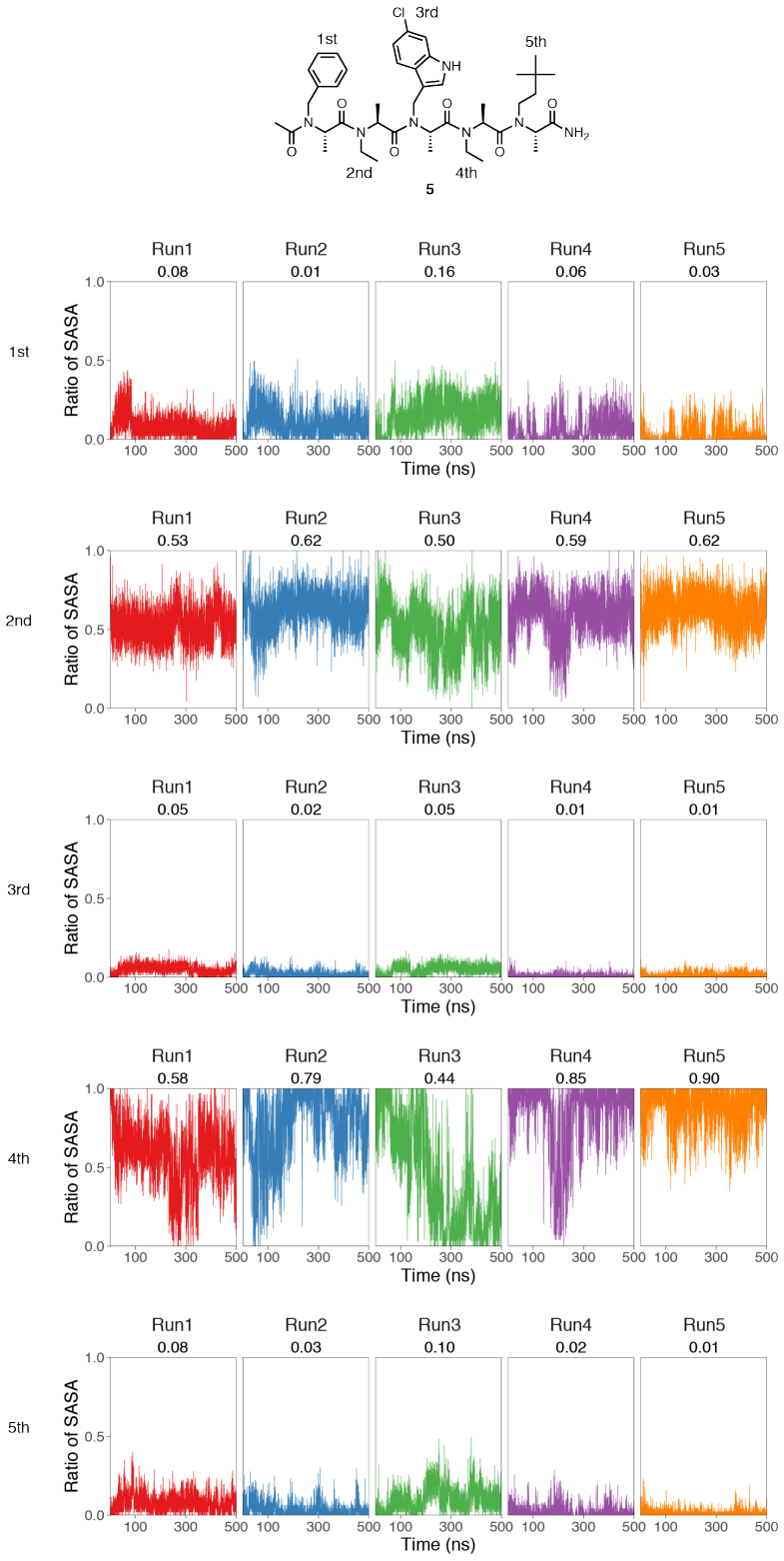

Fig. S26 Ratio of SASA to the whole surface area of each N-substituent during each MD run is plotted. The average during MD run is shown above each plot.

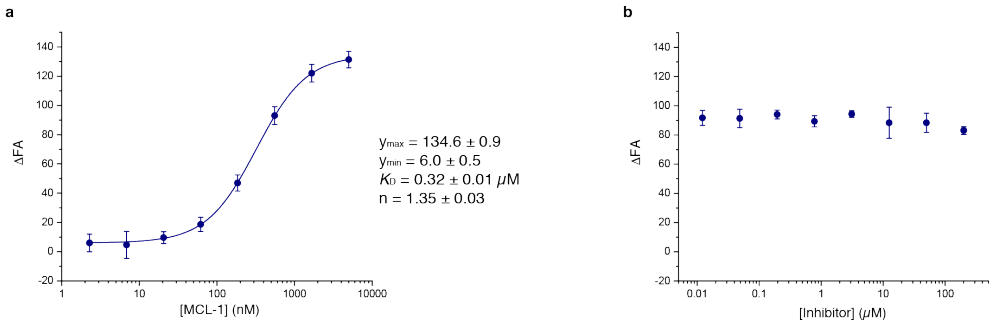

Fig. S27 (a) A binding curve of fluorescently labeled MCL-1 BH3 peptide and MCL-1 generated from FP assay. Error bars represent standard deviations of triplicates. Parameters obtained from the curve fitting (Hill equation: $y = y_{min} + (y_{max} - y_{min})/(1 + (K_D/x)^n)$) of the acquired data are shown. (b) An inhibitory curve of **5** against the interaction between fluorescently labeled MCL-1 BH3 peptide and MCL-1 generated from a competitive FP assay. Error bars represent standard deviations of triplicates.

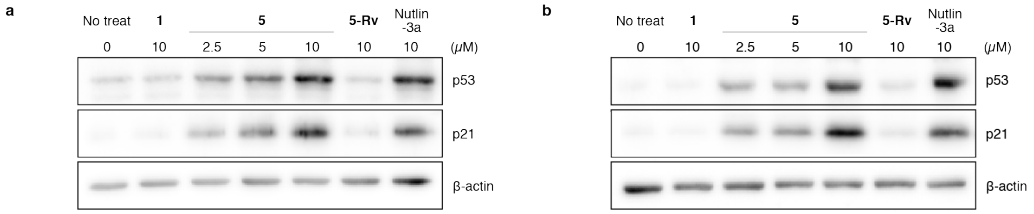

Fig. S28 Intracellular protein levels of p53, p21, and β-actin analyzed by western blotting. SJSA-1 cells were treated with oligo-NSA or Nutlin-3a at the indicated concentrations for 8 h. (a, b) Results of two of three independent experiments are shown. Another result is shown in Fig. 6a.

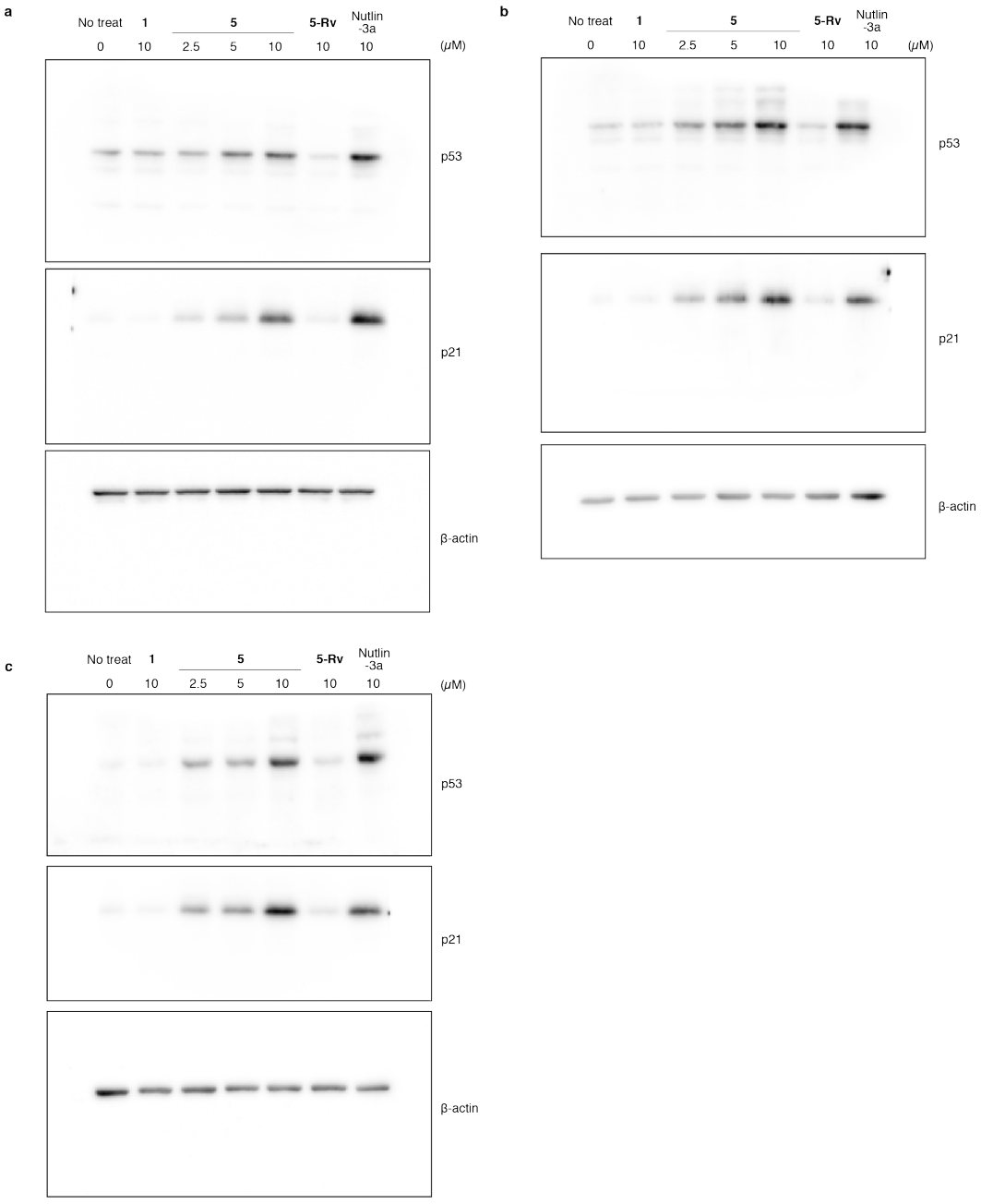

Fig. S29 Uncropped images of Fig. 6a and S28a and b.

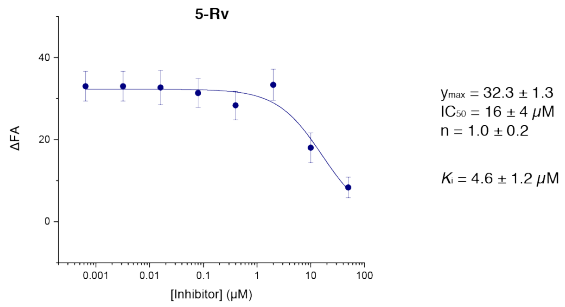

Fig. S30 Inhibitory curves of **5-Rv** against the interaction between fluorescently labeled PMI peptide and MDM2 generated from competitive FP assay. Error bars represent standard deviations of triplicates. Parameters were obtained from the curve fitting (Hill equation: $y = y_{max} - y_{max}/(1 + (IC_{50}/x)^n)$) of the acquired data.

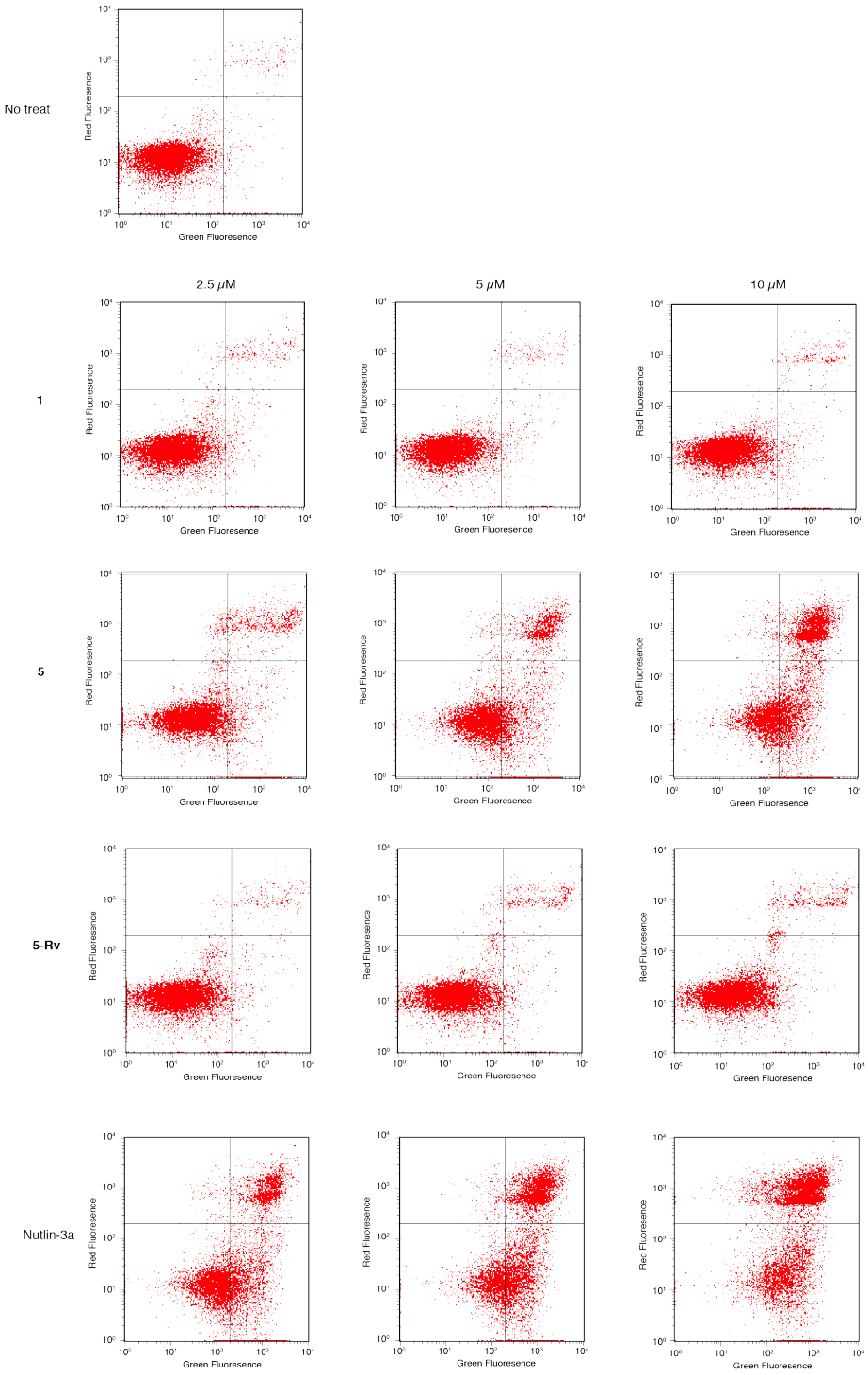

Fig. S31 Measurements of apoptotic SJSA-1 cells by staining with Annexin V-FITC and propidium iodide (PI) (Experiment **1/3**). After the treatment with 0, 2.5, 5, or 10 μM **1**, **5**, **5-Rv**, or Nutlin-3a for 48 h, SJSA-1 cells were labeled with Annexin-V and PI, and analyzed by flow cytometry. Shown is one of the results of three independent experiments.

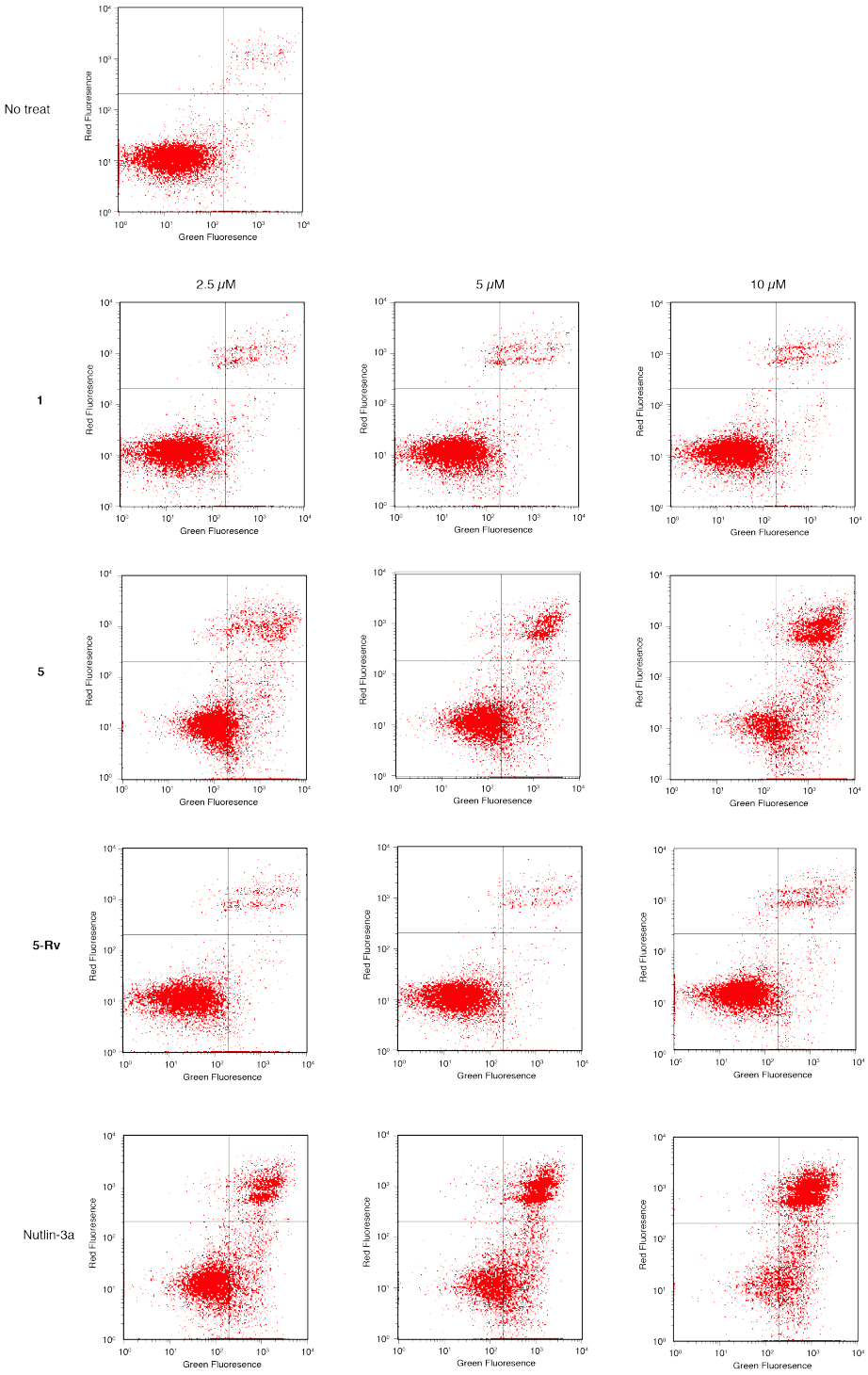

Fig. S32 Measurements of apoptotic SJSA-1 cells by staining with Annexin V-FITC and PI (Experiment **2/3**). After the treatment with 0, 2.5, 5, or 10 μM **1**, **5**, **5-Rv**, or Nutlin-3a for 48 h, SJSA-1 cells were labeled with Annexin-V and PI, and analyzed by flow cytometry. Shown is one of the results of three independent experiments.

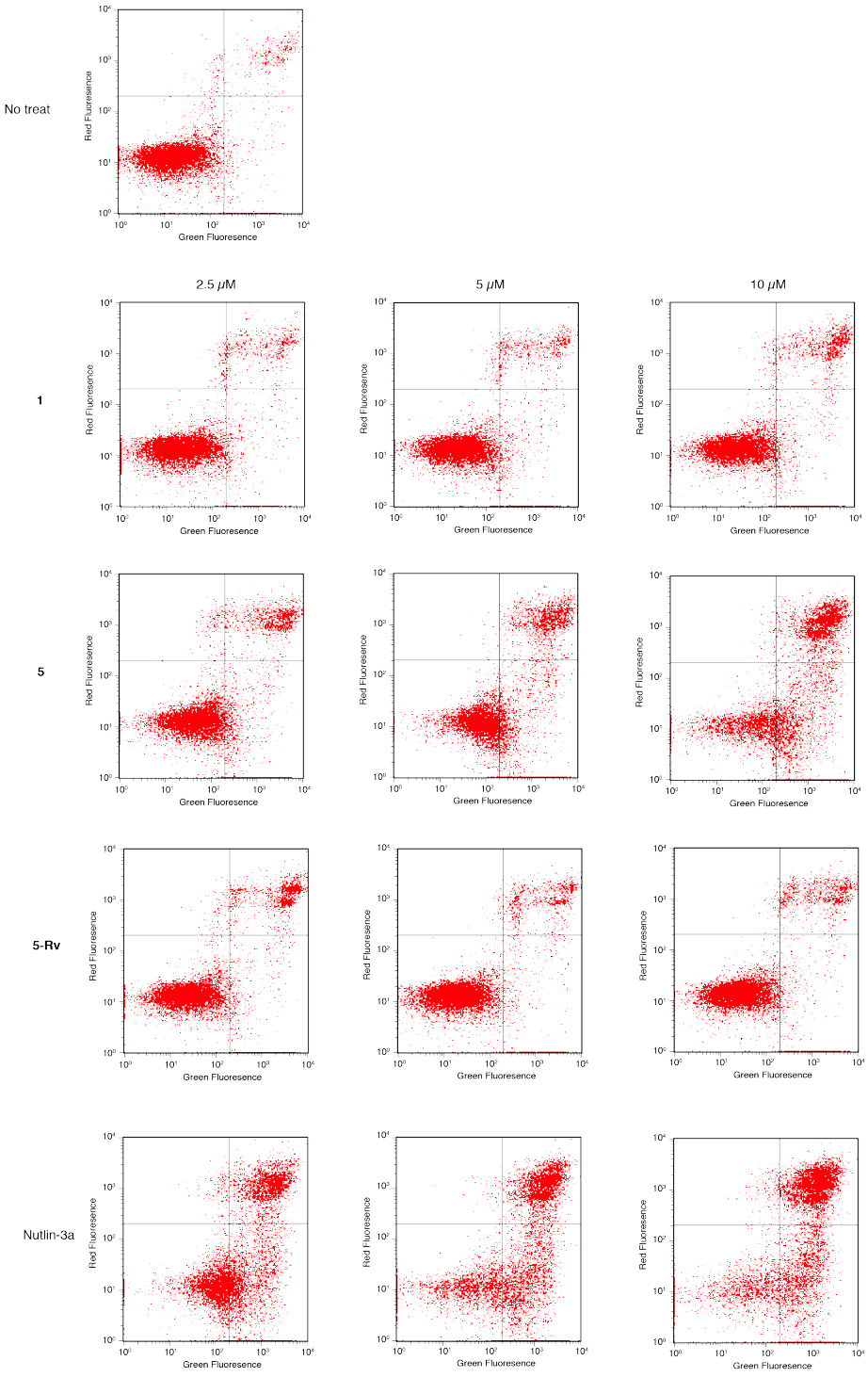

Fig. S33 Measurements of apoptotic SJSA-1 cells by staining with Annexin V-FITC and PI (Experiment **3/3**). After the treatment with 0, 2.5, 5, or 10 μM **1**, **5**, **5-Rv**, or Nutlin-3a for 48 h, SJSA-1 cells were labeled with Annexin-V and PI, and analyzed by flow cytometry. Shown is one of the results of three independent experiments.

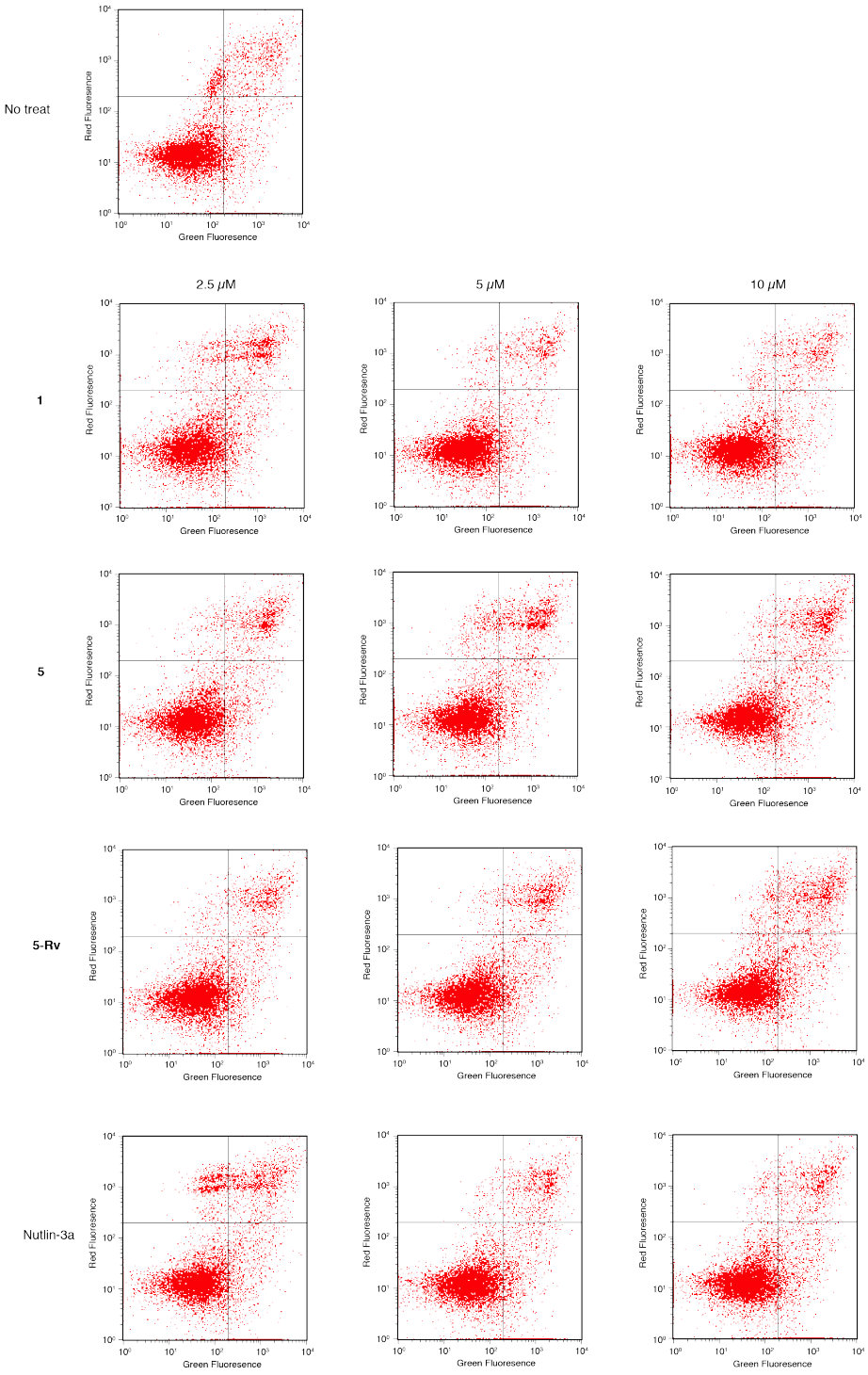

Fig. S34 Measurements of apoptotic SW480 cells by staining with Annexin V-FITC and PI (Experiment **1/3**). After the treatment with 0, 2.5, 5, or 10 μM **1**, **5**, **5-Rv**, or Nutlin-3a for 48 h, SW480 cells were labeled with Annexin-V and PI, and analyzed by flow cytometry. Shown is one of the results of three independent experiments.

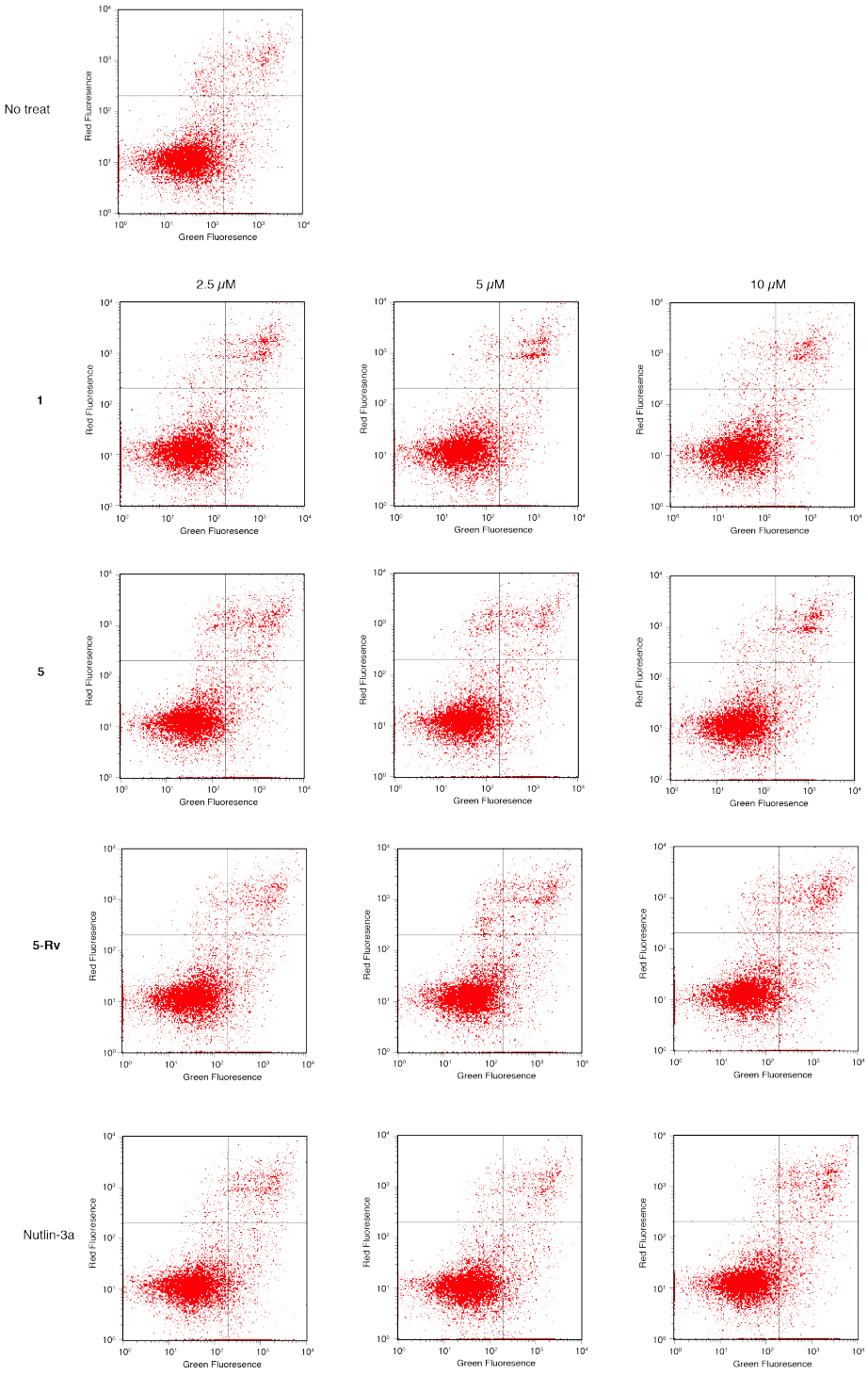

Fig. S35 Measurements of apoptotic SW480 cells by staining with Annexin V-FITC and PI (Experiment **2/3**). After the treatment with 0, 2.5, 5, or 10 μM **1**, **5**, **5-Rv**, or Nutlin-3a for 48 h, SW480 cells were labeled with Annexin-V and PI, and analyzed by flow cytometry. Shown is one of the results of three independent experiments.

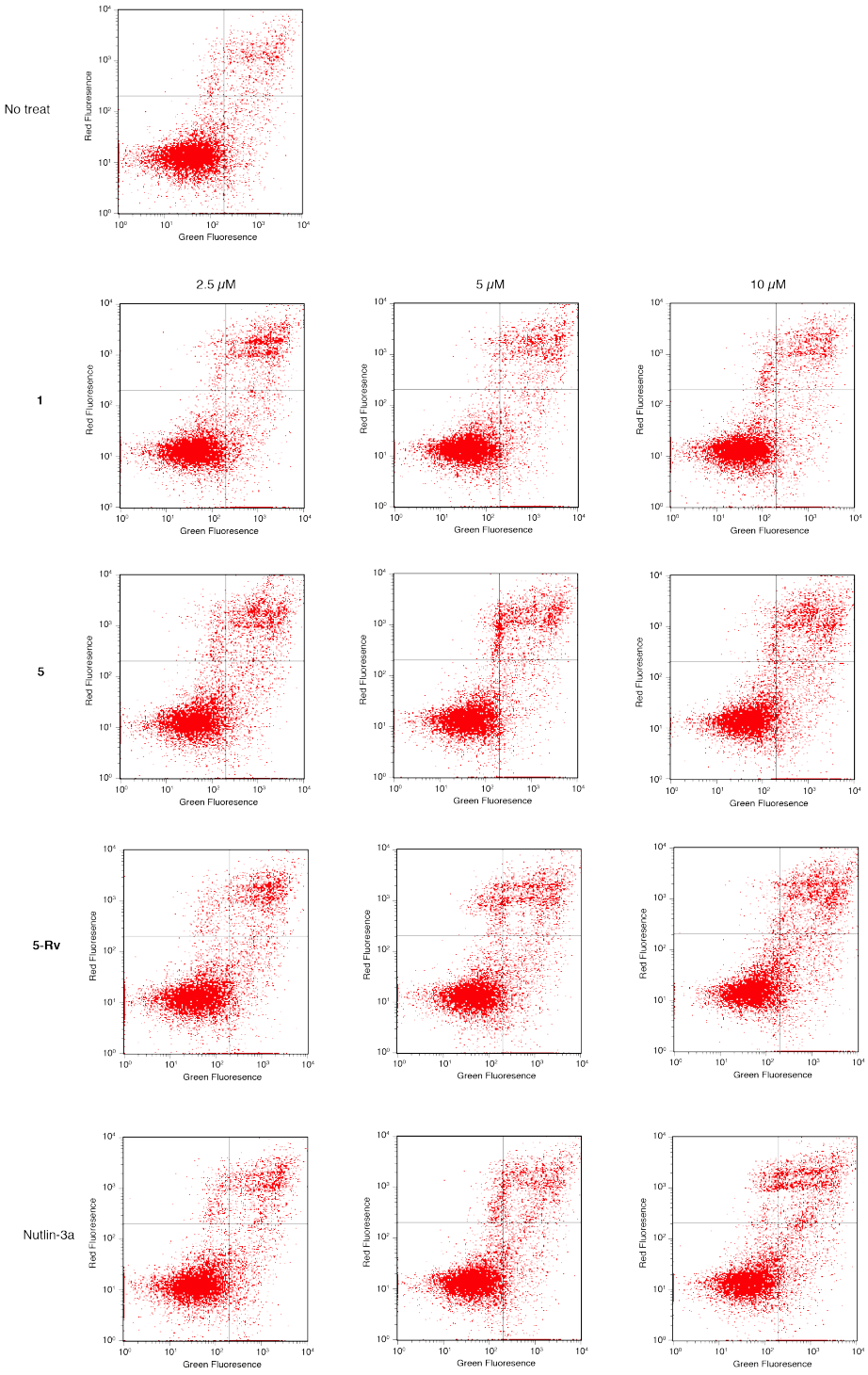

Fig. S36 Measurements of apoptotic SW480 cells by staining with Annexin V-FITC and PI (Experiment **3/3**). After the treatment with 0, 2.5, 5, or 10 μM **1**, **5**, **5-Rv**, or Nutlin-3a for 48 h, SW480 cells were labeled with Annexin-V and PI, and analyzed by flow cytometry. Shown is one of the results of three independent experiments.

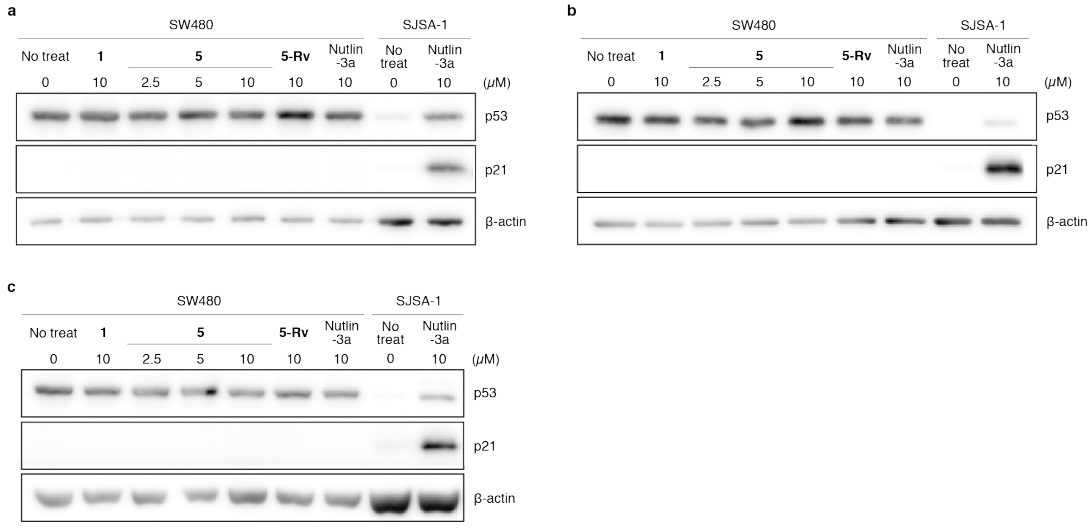

Fig. S37 Intracellular protein levels of p53, p21, and β-actin analyzed by Western blotting. SW480 cells were treated with oligo-NSA or Nutlin-3a at the indicated concentrations for 8 h. (a–c) Results of three independent experiments are shown. As a control, SJSA-1 cells were also treated with vehicle or Nutlin-3a and analyzed.

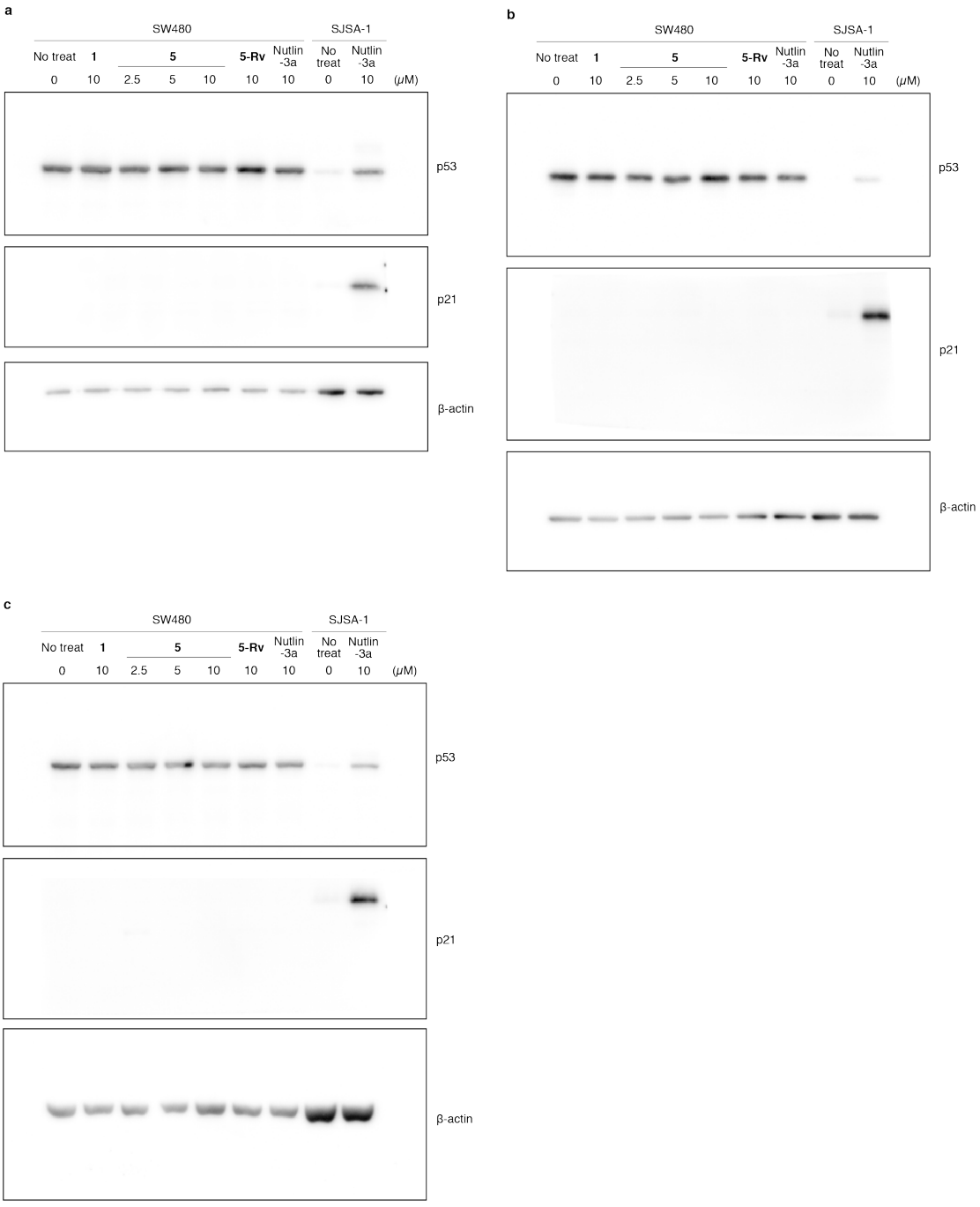

Fig. S38 Uncropped images of Fig. S37.

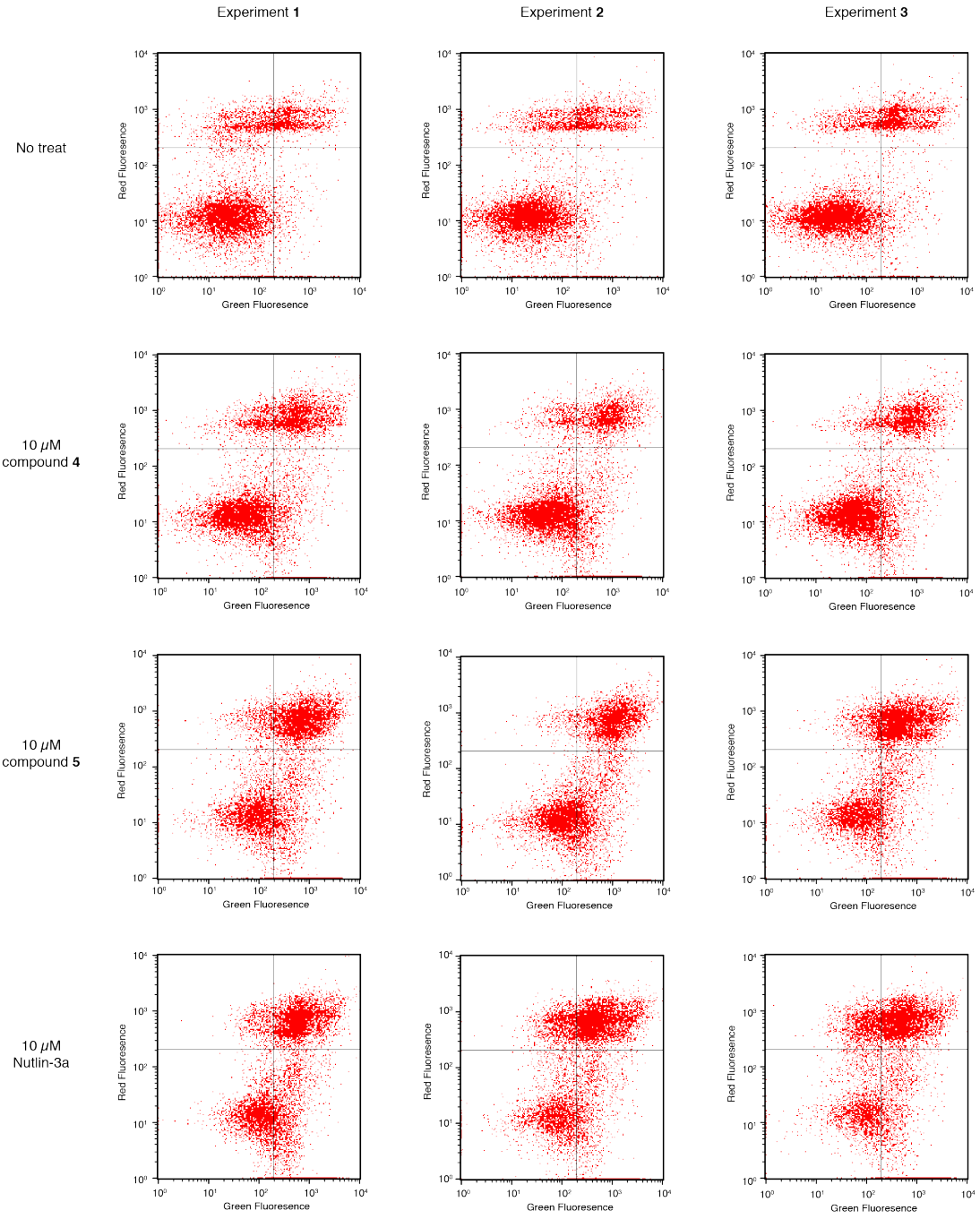

Fig. S39 Measurements of apoptotic SJSA-1 cells by staining with Annexin V-FITC and PI. After the treatment with vehicle or 10 μM **4**, **5**, or Nultin-3a for 48 h, SJSA-1 cells were labeled with Annexin-V and PI, and analyzed by flow cytometry. Results of three experiments are shown.

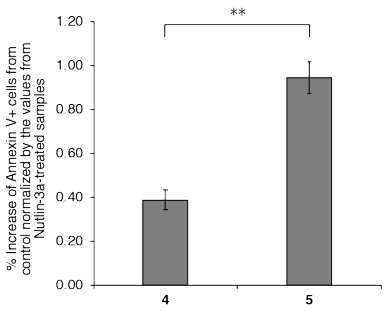

Fig. S40 Apoptotic responses of SJSA-1 cells to 10 μM **4** and **5** measured by Annexin assay. The values of the increase in the ratio of Annexin V-positive cells from the vehicle control were normalized by the values from the samples treated with 10 μM Nutlin-3a. Error bars represent standard deviations of three experiments. **$p < 0.01$ from t test between **4** and **5**.

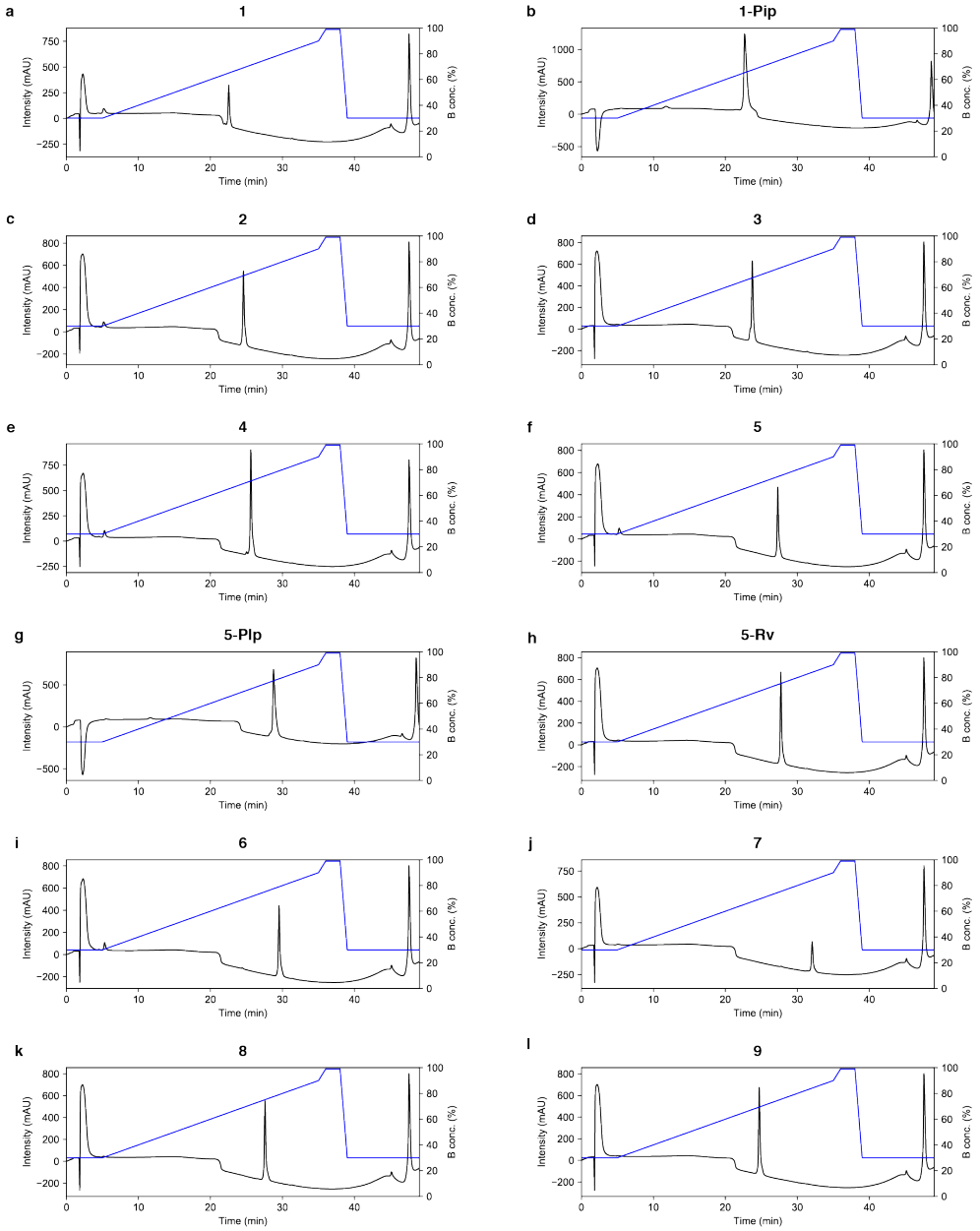

Fig. S41 HPLC chromatograms of compound **1**, **1-Pip**, **2**–**4**, **5**, **5-Pip**, **5-Rv**, and **6**–**9** after purification. Compounds were monitored at 220 nm.

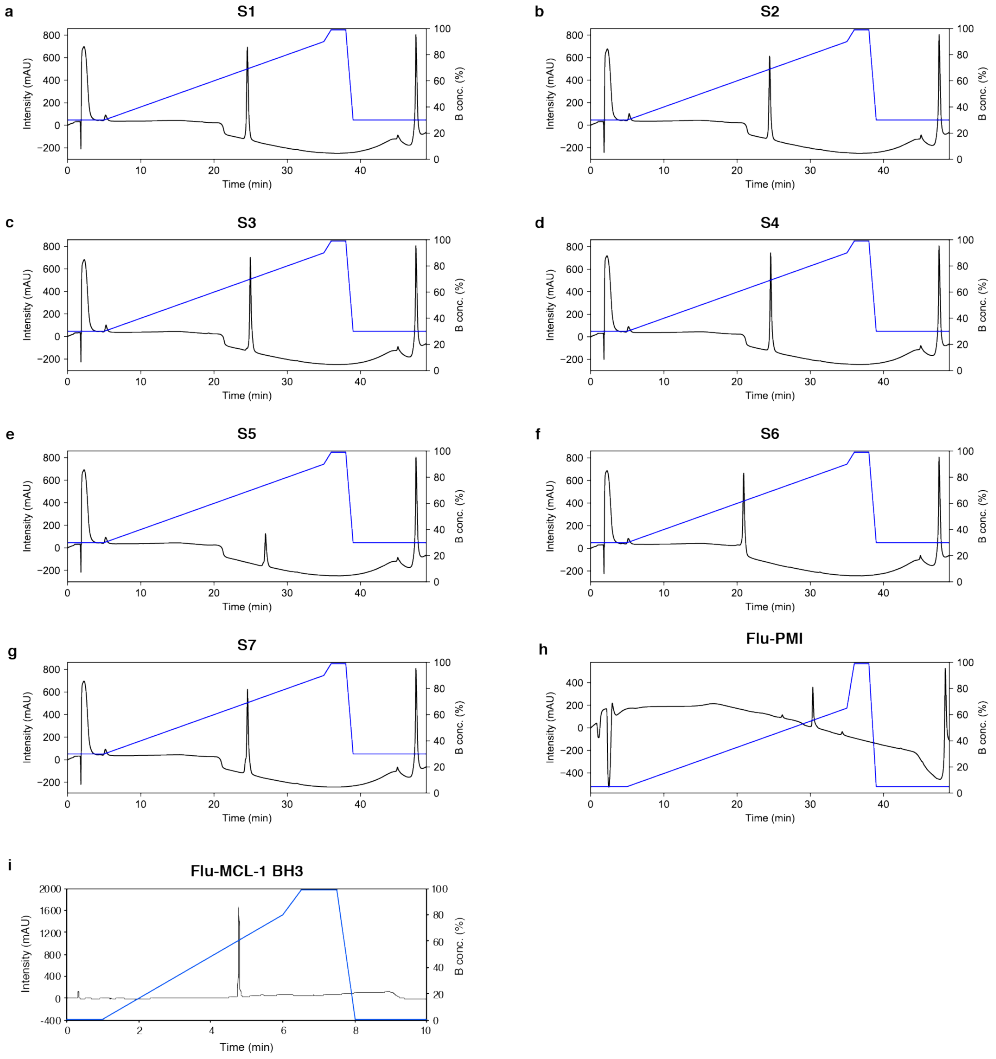

Fig. S42 HPLC chromatograms of compound **S1**–**S7** and **Flu-PMI** (the fluorescence probe used for FP assay) and a UHPLC chromatogram of **Flu-MCL-1 BH3** after purification. Compounds were monitored at 220 nm.

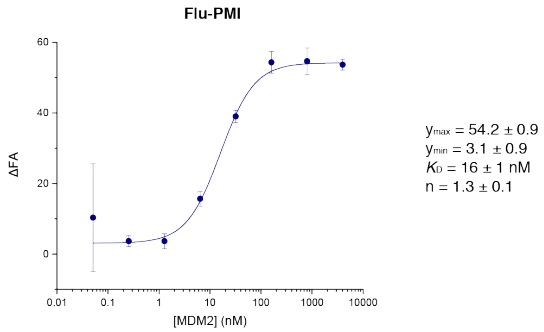

Fig. S43 A binding curve of Fluorescently labeled PMI peptide and MDM2 generated from FP assay. Error bars represent standard deviations of triplicates. Parameters obtained from the curve fitting (Hill equation: $y = y_{min} + (y_{max} - y_{min})/(1 + (K_D/x)^n)$) of the acquired data are shown.

References

1 J. Morimoto, Y. Fukuda, D. Kuroda, T. Watanabe, F. Yoshida, M. Asada, T. Nakamura, A. Senoo, S. Nagatoishi, K. Tsumoto and S. Sando, *J. Am. Chem. Soc.*, 2019, **141**, 14612–14623.

2 G. A. Sable, K. J. Lee, M. K. Shin and H. S. Lim, *Org. Lett.*, 2018, **20**, 2526–2529.

3 M. Pazgier, M. Liu, G. Zou, W. Yuan, C. Li, C. Li, J. Li, J. Monbo, D. Zella, S. G. Tarasov and W. Lu, *Proc. Natl. Acad. Sci.*, 2009, **106**, 4665–4670.

4 W. Borcherds, F. X. Theillet, A. Katzer, A. Finzel, K. M. Mishall, A. T. Powell, H. Wu, W. Manieri, C. Dieterich, P. Selenko, A. Loewer and G. W. Daughdrill, *Nat. Chem. Biol.*, 2014, **10**, 1000–1002.

5 Z. Nikolovska-Coleska, R. Wang, X. Fang, H. Pan, Y. Tomita, P. Li, P. P. Roller, K. Krajewski, N. G. Saito, J. a. Stuckey and S. Wang, *Anal. Biochem.*, 2004, **332**, 261–273.

6 X. Chen, A. Murawski, K. Patel, C. L. Crespi and P. V. Balimane, *Pharm. Res.*, 2008, **25**, 1511–1520.

7 I. V. Tetko, J. Gasteiger, R. Todeschini, A. Mauri, D. Livingstone, P. Ertl, V. A. Palyulin, E. V. Radchenko, N. S. Zefirov, A. S. Makarenko, V. Y. Tanchuk and V. V. Prokopenko, *J. Comput. Aided. Mol. Des.*, 2005, **19**, 453–463.

8 M. J. Frisch, G. W. Trucks, H. B. Schlegel, G. E. Scuseria, M. A. Robb, J. R. Cheeseman, G. Scalmani, V. Barone, G. A. Petersson, H. Nakatsuji, X. Li, M. Caricato, A. V. Marenich, J. Bloino, B. G. Janesko, R. Gomperts, B. Mennucci, H. P. Hratchian, J. V. Ortiz, A. F. Izmaylov, J. L. Sonnenberg, Williams, F. Ding, F. Lipparini, F. Egidi, J. Goings, B. Peng, A. Petrone, T. Henderson, D. Ranasinghe, V. G. Zakrzewski, J. Gao, N. Rega, G. Zheng, W. Liang, M. Hada, M. Ehara, K. Toyota, R. Fukuda, J. Hasegawa, M. Ishida, T. Nakajima, Y. Honda, O. Kitao, H. Nakai, T. Vreven, K. Throssell, J. A. Montgomery Jr., J. E. Peralta, F. Ogliaro, M. J. Bearpark, J. J. Heyd, E. N. Brothers, K. N. Kudin, V. N. Staroverov, T. A. Keith, R. Kobayashi, J. Normand, K. Raghavachari, A. P. Rendell, J. C. Burant, S. S. Iyengar, J. Tomasi, M. Cossi, J. M. Millam, M. Klene, C. Adamo, R. Cammi, J. W. Ochterski, R. L. Martin, K. Morokuma, O. Farkas, J. B. Foresman, D. J. Fox, Gaussian, Inc. Wallingford, CT, 2016.

9 M. J. Abraham, T. Murtola, R. Schulz, S. Páll, J. C. Smith, B. Hess and E. Lindah, *SoftwareX*, 2015, **1**–**2**, 19–25.

10 J. Huang, S. Rauscher, G. Nawrocki, T. Ran, M. Feig, B. L. De Groot, H. Grubmüller and A. D. MacKerell, *Nat. Methods*, 2016, **14**, 71–73.

11 A. Allouche, *J. Comput. Chem.*, 2012, **32**, 174–182.

12 R. López, *J. Cheminform.*, 2014, **4**, 1–17.

13 W. L. Jorgensen, J. Chandrasekhar, J. D. Madura, R. W. Impey and M. L. Klein, *J. Chem. Phys.*, 1983, **79**, 926–935.

14 B. Hess, H. Bekker, H. J. C. Berendsen and J. G. E. M. Fraaije, *J. Comput. Chem.*, 1997, **18**, 1463–1472.

15 T. Darden, D. York and L. Pedersen, *J. Chem. Phys.*, 1993, **98**, 10089–10092.

16 E. F. Pettersen, T. D. Goddard, C. C. Huang, G. S. Couch, D. M. Greenblatt, E. C. Meng and T. E. Ferrin, *J. Comput. Chem.*, 2004, **25**, 1605–1612.

17 L. A. Kelley, S. P. Gardner and M. J. Sutcliffe, *Protein Eng.*, 1996, **9**, 1063–1065.

18 B. Webb and A. Sali, *Curr. Protoc. Bioinforma.*, 2016, **54**, 5.6.1–5.6.37.